Characterisation of Ionic Liquid doped Polybenzimidazole Membranes for Application in High-Temperature Proton Exchange Membrane Fuel Cells

by

Adam Jacobsson Trönndal

Department of Chemical Engineering
Lund University

May 2023

Supervisor: Per Tunestål
Co-supervisor: Annika Carlson, David Aili
Examiner: Christian Hulteberg

Acknowledgement

First of all, I would like to thank RISE and the project HIONIC for allowing me to write my master's thesis with them. Thank you, Annika Carlson and David Aili, for putting up with my lack of knowledge and thank you for guiding me through the complex world of fuel cells and electrochemistry. I have learnt so much and really could not have done it without you. Thank you to DTU for giving me a place to do my experiments and especially thanks to Chao Pan, the lab technician at DTU, for showing me how to do the experiments and helping me do them. Thank you, Anna Martinelli and Eduardo Maurina Morais at Chalmers, for providing me with the material tested. I would also like to thank my university supervisor, Per Tunestål, for giving me valuable insights and comments during the project.

I would like to thank Øresundstågen for taking me to Denmark and (sometimes) being on time and not being cancelled (for the most part).

Lastly, I want to thank my family and friends for supporting me and believing in me my entire academic career. Most of all I would like to thank my girlfriend for putting up with early mornings and a stressed out Adam the last semester. Also, thank you for always bringing a smile to my face. You have given me the strength to get through this with my sanity intact.

Thank you all!

Abstract

In this study four membranes were tested and evaluated against each other for use in high-temperature proton exchange membrane fuel cell (HT-PEMFC) applications. A phosphoric acid (PA) doped polybenzimidazole (PBI) membrane, was used as a reference as the current state-of-the-art. The charge carrier in this membrane is the PA, and there are advantages in switching from PA to ionic liquid (IL) as the charge carriers in HT-PEMFC, such as to reduce leaching and lost performance over time. Two of the membranes investigated in this study were PBI mixed with the commercial ILs [dema][TfO] and [HEIm][TFSI]. The last membrane was a mixture of PBI and a newly synthesized IL by Chalmers University of Technology, [FA][TFSI]. Conductivity measurements, polarisation curves and electrochemical impedance spectroscopy (EIS) were done to characterise and evaluate the membranes.

The study shows that these IL-PBI membranes have a long way to go to be a commercially competitive technique compared to PA-PBI membranes. In the report it can be seen that all the IL-PBI membranes show very poor performance without the addition of PA. Even with the addition of PA, the performance of the IL-PBI membranes cannot compare to PA-PBI membranes, being a factor 10 lower in the conductivity test and polarisation curves. In the EIS the membrane that got a conductivity closest to PA-PBI was [FA][TFSI]-PBI that had a conductivity that was 70% of the conductivity of PA-PBI. The lower performance for the membranes in the polarisation measurements compared to the EIS can be due to several factors such as changed membrane resistance with applied load or the influence of other cell resistances. Tests where the membranes were doped with the corresponding IL in the electrodes instead of PA also showed poor performance.

Future studies in the field of IL-PBI membranes are needed for the technology to become viable as an alternative to PA-PBI.

Sammanfattning

I denna studie testades och utvärderades fyra membran mot varandra för användning i högtemperaturprotonutbytesmembranbränslecell (HT-PEMFC) applikationer. En fosforsyra (PA)-dopat polybensimidazol (PBI)-membran användes som en referens som den nuvarande state-of-the-art. Laddningsbäraren i detta membran är PA, och det finns fördelar med att byta från PA till jonisk vätska (IL) som laddningsbärare i HT-PEMFC, som att minska urlakning och förlorad prestanda över tid. Två av membranen som undersöktes i denna studie var PBI blandat med de kommersiella ILs [dema][TfO] och [HEIm][TFSI]. Det sista membranet var en blandning av PBI och en nysyntetiserad IL av Chalmers tekniska högskola, [FA][TFSI]. Konduktivitetsmätningar, polarisationskurvor och elektrokemisk impedansspektroskopi (EIS) gjordes för att karakterisera och utvärdera membranen.

Studien visar att dessa IL-PBI-membran har en lång väg att gå för att vara en kommersiellt konkurrenskraftig teknik jämfört med PA-PBI-membran. I rapporten kan man se att alla IL-PBI-membran uppvisar mycket dålig prestanda där PA inte är tillsatt. Även med tillägg av PA kan IL-PBI-membranens prestanda inte jämföras med PA-PBI-membranen, eftersom de är en faktor 10 lägre i konduktivitetstestet och polarisationskurvorna. I EIS var det membran som fick en konduktivitet närmast PA-PBI [FA][TFSI]-PBI som hade en konduktivitet som var 70% av PA-PBI. Den lägre prestandan för membranen i polarisationsmätningarna jämfört med EIS kan bero på flera faktorer såsom förändrat membranresistans med applicerad belastning eller påverkan av andra cellresistanser. Tester där membranen dopats med motsvarande IL i elektroderna istället för PA visade också dålig prestanda.

Framtida studier inom området IL-PBI-membran behövs för att tekniken ska bli livskraftig som ett alternativ till PA-PBI.

Table of Contents

1 Introduction

There is an array of interesting electrochemical technologies that have promising prospects for the future, including batteries, super capacitors, and fuel cells. In conjunction with various power-to-X technologies these could be vital for the energy transition in society today. An increasing knowledge in these areas is, however, needed to make these technologies commercially competitive to the sources that are dominating on the energy market today, which is mainly fossil fuel driven. In the case of light-duty vehicles application today the dominating electrochemical energy converter technology is batteries, but the low temperature proton exchange membrane fuel cell (LT-PEMFC) has gotten some attention lately because of its high power density and has started to be used in light duty vehicles. A higher temperature could solve some problems that LT-PEMFC have like CO-poisoning from fuel or oxidant impurities and also increase conductivity without dependence on water. This has led to that high temperature PEMFC (HT-PEMFC) have gotten some attention. HT-PEMFC has a relatively high efficiency, is light weight and have zero greenhouse gas (GHG) emissions. HT-PEMFC also have easier water management due to operating at temperatures much above the boiling point of water and avoiding condensation. HT-PEMFC uses phosphoric acid (PA) in polybenzimidazole (PBI) as its electrolyte and conductivity is not dependent on water. However, PA-PBI has its own complications. Acid leaching is one problem that can result in gradual degradation of cell performance so an alternative to PA as an electrolyte in HT-PEMFC is of interest. Additionally, PA strongly adsorbs to the platinum electrocatalysts, which results in large activation overpotential. If the problems with HT-PEMFC can be solved they are to be believed to be a potential alternative to LT-PEMFC and batteries at replacing fossil fuel driven combustion engines in the future, at least for long distance applications or as methanol-fuelled range extenders for battery electric vehicles. One way of replacing PA in HT-PEMFC could be to use ionic liquids (IL) in membranes.

HT-PEMFC could help the world to achieve zero emission in the future. When looking at the UN sustainable development goals this project can be included in:

- **goal 7:** affordable and clean energy
- **goal 11:** Sustainable cities and communities
- **goal 13:** Climate action

When the infrastructure is in place to support fuel cells, this includes green production of hydrogen, fuelling stations and vehicle application, the technology can produce clean energy at any time needed. By replacing combustion engine driven cars for fuel cell electric vehicles (FCEV) a more sustainable society can be achieved.

1.1 Project description

RISE has together with Chalmers University of Technology, Danish Technical University, Blue World Technologies, Catator, Liquid Wind AB and Volvo AB started the project HIONIC. This project is aimed to characterising a new membrane containing an IL, casted at Chalmers University of Technology by Martinelli and Maurina Morais. In addition, the project aims to increase the knowledge of HT-PEMFC in Sweden. The membrane casted at Chalmers is made of polybenzimidazole (PBI) together with a new IL as the charge carrier. This project is therefore also a way to increase the knowledge in the subject of IL-PBI membranes and evaluating the feasibility to use these in HT-PEMFC in the future.

1.2 Aim

The projects' objective is to test and evaluate a new IL-PBI membrane brought forth by Martinelli and Maurina Morais at Chalmers University of Technology. More specifically, the aim is to evaluate the IL-PBI membrane for the application in HT-PEMFC. The IL-PBI membrane made by Martinelli and Maurina Morais will be evaluated against membranes using commercial IL doped PBI membranes as well as the current state of the art HT-PEMFC using PBI membranes doped with PA as electrolyte.

1.3 Scope

This report will explore the technical feasibility of a new IL doped PBI membrane developed at Chalmers, N-ethyl-N-(furan-2-ylmethyl)ethanaminium bis(trifluoromethylsulfonyl)imide ([FA][TFSI]), for the intended use in HT-PEMFC. Evaluation of the new membrane will be done by comparing polarisation curves, electrochemical impedance spectroscopy measurements and conductivity tests of the new membrane to PBI membranes made with commercial IL as well as PBI membranes doped with PA. The other IL-PBIs used as a comparison in the report is 1-ethylimidazolium bis(trifluoromethylsulfonyl)imide ([HEIm][TFSI]) and diethylmethylammonium triflate ([dema][TfO]) in PBI membranes. The effect of temperature on the conductivity and resistance of the different temperatures will also be evaluated.

2 Background

2.1 Environmental Aspects

The world today is facing an increasing environmental threat where the human contribution to global warming and climate change is noticeable and substantial. [1] There are several factors that are contributing to global warming, but the leading cause is the use of fossil resources. These releases carbon dioxide (CO_2) into the atmosphere when burned. [2] An effort to combat climate change is needed not to destabilise ecosystems and risk human life. One way to do this is to substitute the non-renewable fossil fuel that is used in vehicles today with a more sustainable and environmentally friendly fuel. On such alternative is using hydrogen gas, or other energy carriers that are produced in a renewable way, in fuel cells. [3] Today the transport sector stands for about 16% of the total global greenhouse gas emissions and stood for 8.22 billion tons CO_2 emission in 2019. [4] This is the largest sector of c emissions in the world except for heat and electricity. Because of that Sweden has a lot of green energy production today, the transport sector is the largest contributor to Sweden's CO_2 emission, 16.3 million tons per year. [4] By reducing the amount of fossil fuelled vehicles in society, a large proportion of the worlds, and especially Sweden's, CO_2 emissions could be reduced. There is a large amount of focus into developing electrical vehicles (EV) where the largest market today is the battery EV (BEV). There is research into fuel cell EV (FCEV) as well which has increased in the past years and companies like Hyundai and Toyota have already launched FCEV vehicles with companies like Volvo Group also exploring the possibilities of launching in the upcoming years. [5-7]

The United Nations (UN) as well as the European Union (EU) has brought forth strategies to combat global warming. The EU has said that 15% of the total CO_2 emissions come from cars and trucks today. [8] The EU has put up a goal to reduce the CO_2 emissions from cars and trucks by half by 2030 and with that issued new resources for battery and hydrogen fuelling stations. [8] The UN have brought forth the Sustainable Development Goals (SDG) that aim to guide nations, companies and people to create a better, sustainable society. [9] Both of the UN and the EU hold fuel cells as a good alternative for the future.

2.2 Fuel Cells

Fuel cells are a collection of electrochemical cells that convert chemical energy to electrical energy. It is in theory fairly similar to how batteries work except that batteries have the fuel stored in the electrodes while fuel cells get a continuous input of fuel from an external tank.

The research of fuel cells started as early as the 19th century and the technology has in the latest 30 years gotten increased attention and it is today viewed as a key technology as a future energy converter. It is especially possible to use them to replace combustion engines, but other applications are also investigated. There are many subcategories under the umbrella of the term fuel cells and following will be an introduction to these and discussed shortly.

In a fuel cell a reactant gets oxidised at the anode side and a reactant gets reduced at the cathode side. The ions move through the electrolyte while the electrons move through an external circuit, producing electricity. [10]

Following will be a short presentation of some of the fuel cell types that have been explored as of today. There will be mentions of efficiency of the different types. These are calculated as the percentage of energy received divided by the theoretical chemical energy, so called conversion

efficiency, and does not consider the energy losses from creating the fuel and storing it. These are substantial losses and should be considered when analysing the efficiency of the entirety of fuel cells. [10] However, in this chapter only the different kinds of fuel cells are compared with each other and will therefore not consider energy losses in fuel production.

Phosphoric Acid fuel cells (PAFC) is an old, mature technology in the field of fuel cells and was one of the first fuel cells to be researched on. The catalyst used in PAFC is usually platinum which makes it an expensive technology. The operating temperature is 150-200℃ and the efficiency is low, 40-50%, which makes this technology less interesting for the future. However, operating at higher temperature improves catalyst kinetics and improves tolerance to CO poisoning. PAFC is, as previously said, a mature, reliable technology which is why it is often used as back-up generators in places like hospitals and airports. [10]

Molten Carbonate fuel cells (MCFC) use a melt of lithium-, sodium- and potassium carbonates as an electrolyte. This melt is corrosive which can cause problems in applications. MCFCs operating temperature is 650℃ and the energy efficiency is about 60%. [10] The higher operating temperature allows a cheaper catalyst, mostly used is Nickel (Ni), and still has a high conversion rate. Likewise, integrating the fuel cell with a steam generator can increase the efficiency of the fuel cell. However, the high operating temperature can be damaging to the fuel cells components. Nickel is also the basis of the electrode. [10] MCFC can use a wide range of fuels and not constricted to hydrogen- and oxygen gas.

Solid Oxide fuel cells (SOFC) operate at a distinctively higher temperature, 650℃-800℃. The high operating temperature allows for the reactions to take place without catalysts but operating at such high temperatures can be expensive and can make the fuel cell unstable. Ni is sometimes used as a catalyst. Also, the high operating temperature can also affect and damage the fuel cells components. The electrolyte in the case of SOFC is a solid, hard oxide ceramic material and the fuel can either be hydrogen or natural gas could also be used directly. Due to the high operating temperature a steam turbine can be integrated to generate electricity of the product water to increase the efficiency. Without integration the efficiency is 60%. [10]

Alkaline fuel cells (AFC) are a type of fuel cell that is not dependent on platinum as a catalyst as most other fuel cell types are which is a definite advantage of the AFC. This is since platinum is an expensive and finite resource. AFCs uses potassium hydroxide (KOH) as the electrolyte and has an energy efficiency of 70% [10] and operates under 100℃. [11] A disadvantage of AFCs is that the feed at the cathode needs to be free from CO_2 since it creates $NaHCO_3$ and CO_3^{2-} when reacting with KOH which lowers the conductivity. This means that either CO_2 free air or pure oxygen feed is required. AFCs have been used in spacecrafts. [10]

Polymer electrolyte fuel cells (PEFC) can be divided into hydrogen fuel cells, using a feed of hydrogen gas as fuel, direct methanol fuel cells and direct ethanol fuel cells, using methanol respectively ethanol together with water as fuel. In common for all of them is that they use a solid polymer membrane as electrolyte.

Direct Methanol fuel cells (DMFC) and Direct Ethanol fuel cells (DEFC) are fuel cells where alcohol and water are used as a fuel and react directly at the anode with the catalyst to produce the protons. By-products are CO_2 and CO which exit with the unreacted alcohol and water. The advantage of this is that you do not need a reformer before the fuel cells that convert the alcohol to hydrogen and therefore do not lose the efficiency of the conversion. This makes the technology viable even though the efficiency of the DMFC and DEFC are 30-40%. Operating temperature is 50-100℃. [10]

Proton Exchange Membrane fuel cells (PEMFC) can be divided into low- (LT-PEMFC) and high-temperature (HT-PEMFC). LT-PEMFC is the oldest of these and was one of the first fuel cell types to be commercialised. LT-PEMFC usually uses a Nafion® membrane. LT-PEMFC is optimally operating around 80℃ and is dependent on water for the ion conductivity. It can therefore have problems with water management as well. If water is not removed optimally the cell loses efficiency and since water is both removed and created in the process, there can be too little and too much water in the system. Either the membrane can flood with too much water, or the membrane can dry out if too much water gets removed. This is one on of the reasons alternatives to LT-PEMFC are being investigated. HT-PEMFC operates at a higher temperature, optimally 160℃, which solves much of the water problem. HT-PEMFC also has a higher efficiency than LT-PEMFC since LT-PEMFC has an efficiency of energy conversion of about 50-60% [10] whilst HT-PEM usually has an energy efficiency of >60%. [12] As previously stated, LT-PEMFC mostly use Nafion® membranes today, but the thermal and chemical stability is not sufficient for long term use at higher temperatures. Therefore, a search for a better membrane alternative for HT-PEMFC was needed and today most HT-PEMFC uses PBI membranes.

The largest difference between HT-PEMFC and LT-PEMFC is the operating temperature, where HT-PEMFC runs around 160℃ whilst LT-PEMFC runs at around 80 ℃. With this follows some fundamental differences. In HT-PEMFC, the water is vapour and cannot conduct ions. This had led to HT-PEMFC to uses other electrolytes like phosphoric acid (PA) or different IL that are in liquid state at these temperatures. [13] As previously said, LT-PEMFC has for a long time used a proton conducting membranes called Nafion® because of its excellent proton conducting ability and mechanical strength. However, Nafion®s ability to conduct protons rely on water being present and when Nafion® is used in HT-PEMFC, where the temperatures are >100℃, Nafion® membranes dry out and cannot operate. [3,11]

Table 1. A summary of fuel cells and their electrolyte, operating temperature, electrical efficiency and fuel composition.

Fuel cell name	Electrolyte	Operating temperature [℃]	Electrical efficiency	Fuel mixture
Phosphoric Acid fuel cells (PAFC)	Phosphoric acid	150-200	40-50%	H_2 – air (or O_2)
Molten Carbonate fuel cells (MCFC)	Molten mixture of alkali metal carbonates	650	60%	Natural gas, biogas, coalgas, H_2 – air (or O_2)
Solid Oxygen fuel cells (SOFC)	Oxide ion conducting ceramic	650-800	60%	Natural gas, biogas, coalgas, H_2 – air (or O_2)
Alkaline fuel cells (AFC)	Potassium hydroxide (KOH) solution	<100	70%	H_2 – CO_2 (scrubbed air)
Direct Methanol- and Direct Ethanol fuel cells (DMFC/DEFC)	Perfluorosulfonic acid membranes	50-100	30-40%	CH_2OH/C_2H_5OH – O_2 or air
Low-Temperature Proton Exchange	Perfluorosulfonic acid membranes	80	50-60%	H_2 – air (or O_2)

Membrane fuel cells (LT-PEMFC)				
High-Temperature Proton Exchange Membrane fuel cells (HT-PEMFC)	Phosphoric acid doped polymer membranes	160	>60%	H_2 – air (or O_2)

This report will further focus on HT-PEMFC, and no other concepts will be covered in more detail.

2.2.1 Hydrogen storage

A major concern for future applications of fuel cells is the volume needed for the storage of the fuel. This is because of hydrogens low energy density. The US Department of Energy [14] have calculated that a FCEV that was run on hydrogen and had a pressurised hydrogen tank of 700 bar would need a 200 L tank, which is more than 3 times that of a diesel tank today. Heavy-duty trucks, as of today, usually uses 350 bar tanks to store the hydrogen. Gittleman et. al. [3] states that if this would be the case, trucks that today have an 800 L gasoline tank would need a 7800 L hydrogen storage tank if switched to hydrogen driven fuel cells. If you use methanol, or other liquid fuel, as a fuel with a converter instead, the tank can be reduced to 2460 L which is better than the compressed hydrogen storage but still considerably larger than the gasoline tank of today. [3] This is an area that needs some development to make fuel cells commercial in the future. Another advantage of liquid fuel over compressed hydrogen is that the infrastructure for liquid pumping and distribution already exists and needs little to no changes. If fuel cells combine with a converter, methanol could be used as fuel which could use the existing infrastructure with small adjustments. Shih et.al. [15] projected that the cost of the infrastructure needed for compressed hydrogen would cost $15 trillion while most infrastructure for methanol distribution already exists which would put the cost of adjusting the existing infrastructure for this new purpose at just $50 billion. The infrastructure of liquid fuels is also less than that of the electric batteries which is $5 trillion, mainly due to the need for grid expansion.

2.3 High-Temperature Proton Exchange Membrane Fuel Cells

2.3.1 General about HT-PEMFC

HT-PEMFC consists of different layers. From anode side to cathode side, they are as bipolar plate, gas diffusion layer (GDL), anode electrode, membrane, cathode electrode, GDL and bipolar plate, see Figure 1. The bipolar plates collect electrons released from the electrochemical oxidation reaction at the anode and allow them to move to the cathode electrode by the external circuit. The GDL in HT-PEMFC are often made of carbon fibre paper that has good porosity as well as good heat- and electric conductivity. This carbon fibre paper is often treated with poly-tetra-fluoro-ethylene (PTFE) to make the material hydrophobic, ensuring that the pores do not get filled with water. [10] The electrochemical kinetics is determined by the mass transfer from the bulk through the GDL. Therefore, the electron transfer is also determined by the mass transfer of reactant. The catalyst then gets sprayed upon the GDL to get a good contact between reaction site and the GDL. [16] When the fuel has gone through the GDL, it reacts at the catalyst active sites, producing protons and electrons. Through the membrane no electrons nor non-ions can travel, and in the case of HT-PEMFC it is only protons that travel through. The layers mirror on the cathode side. A simple illustration can be seen in Figure 1.

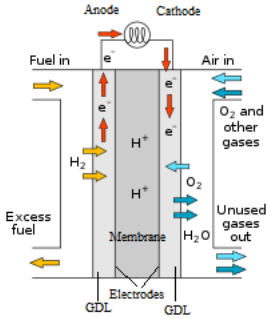

Figure 1. A simple illustration of a HT-PEMFC.

2.3.2 Advantages and Application of HT-PEMFC

The interest for HT-PEMFC has increased in recent years especially because of its interesting prospects in heavy-duty vehicles. The advantages of HT-PEMFC are its high energy efficiency and power density, low emissions, its light weight and compact size, fast start-up, relatively low operating temperature and low refuelling time. The high temperature also increases the kinetics of the reaction by improving catalyst efficiency and higher temperature makes the cell more resilient to CO poisoning. [17]

In vehicles, HT-PEMFC would allow for the fuel cells systems to have simpler thermal management and water elimination which would be a distinct advantage over the LT-PEMFC. It has been shown that operating fuel cells under high temperatures and dry conditions could improve catalytic ability, improve oxygen transfer, and reduce the Pt oxide formation. Gittleman et.al [3] says that these are all effects of removing water from the systems that often cause problems in LT-PEMFC when not being handled well. Gittleman et.al [3] also states that by operating fuel cells over 100°C enables the exploitation of latent heat systems where the coolant changes stage which gives a higher heat capacity than if the coolant remains in the same stage. This allows smaller radiators and a lower wind drag design.

2.3.3 Disadvantages and Problems with HT-PEMFC

At this point, the state of the art of HT-PEM fuel cells is using a Pt catalyst and PA-PBI membrane which show great thermal-, chemical-, and mechanical stability at high temperature. However, a long-term concern is that Pt is a noble metal, found in authoritarian countries, mainly South Africa but also Russia, and has a considerable cost. It accounts for about 55% of the cost of a HT-PEMFC today. [16]

Pingitore et.al [18] found that PA-PBI membranes in HT-PEMFC could have a stable operation for over 17,000h at 160°C and Kannan et.al [19] showed stable operation for over 10,000h at 180°C. However, when looking at operation under 140°C the performance worsened, and the fuel cells did not have the same stability. This was attributed to the loss of phosphoric acid in the presence of water in the cell which can occur at lower temperatures. [3] Therefore, the operating temperature for PA-PBI HT-PEMFC is today set at 160°C and to achieve higher temperature in application, a high-power battery is needed to heat the fuel cell at start-up to not damage the cell. Over 160°C PA can evaporate which again can lower the performance. However, when operating HT-PEMFC at optimal conditions the fuel cell can generate more energy than what is needed which can charge the battery while driving which can solve some of these problems. [3]

Another problem with HT-PEMFC that needs to be solved when using PA-PBI membranes is that PA leaks from the membrane over time which can damage the cell. An alternative to PA in HT-PEMFC is IL that could give better prospects for long term use.

2.3.4 Anode

At the anode in a HT-PEMFC the fuel, which is hydrogen gas, gets oxidised in a hydrogen oxidation reaction (HOR). This reaction produces protons as well as electrons, see *reaction 1*.

$$H_2 \rightarrow 2H^+ + 2e^- \quad (1)$$

The activation energy of this reaction is normally high, and the reactions are non-spontaneous. A catalyst is needed to get the reactions to take place and the most common catalyst in HT-PEMFC today is platinum. The half-cell potential at the anode is E^0=0V.

2.3.5 Cathode

The cathode side of a HT-PEMFC is the electrode that is responsible for the reduction of the oxidant, the oxygen reduction reaction (ORR). The fuel on the cathode side is oxygen and this reacts with the electrons and protons provided by the anode side to form water, see *reaction 2*. The cathode in HT-PEMFCs has a higher activation energy than the anode side so a catalyst is needed also here. Platinum is the most used catalyst.

$$\frac{1}{2}O_2 + 2H^+ + 2e^- \rightarrow H_2O \quad (2)$$

When the ions and electrons react, this creates a charge density difference between the anode and cathode which further enables the flow of the electrons and protons from the anode to the cathode. The half-cell potential at the cathode is E^0=1.23V.

2.3.6 Electrolyte

In HT-PEMFC the membrane needs to be doped with a charge carrier since the membranes that are stable at temperatures higher than 100°C rarely have sufficient proton conductivity. The state of the art in HT-PEMFC today uses PBI membranes doped with PA, acting as the charge carrier. In the electrolyte, protons get transported via either Grotthuss or vehicle mechanism. In Grotthuss mechanism the protons get passed along the charge carriers and the membrane structure from the anode side over to the cathode side. In vehicle mechanism the protons get transported by the charge carriers from the anode side to the cathode side. Both mechanisms work due to charge/concentration differences between the two sides. This is the driving force. In vehicle mechanism there is need for diffusion back by the charge carrier which can result in electrolyte imbalance. [16]

2.3.7 Proton conductivity/Ion transport

The proton conductivity through the membrane is one of the charge transports that happen in a fuel cell. The other one is electron transport. However, electron transport is much easier because charge transport is dependent on mass and the typical mass difference between ions and electrons is very large. Therefore, the electron transport can be done using electron conducting materials, like many metals that cannot conduct protons and other ions. [10] In fuel cells there is a potential difference between the electrodes which creates the driving force of electrons to go through the external circuit, creating the current. Therefore, it is paramount that the membrane is electronically insulating to have the electrons to go through the external circuit instead of through the membrane. On the other hand, the ions migrate through the electrical

field between the anode and cathode, which results in migration from the anode to the cathode through the membrane.

Since electrons and protons react at the cathode, creating water that gets exhausted from the cathode side, the driving force remains, and the transport is spontaneous. [10] If a pressure gradient is put over the membrane, this could also affect the ion migration through the membrane and if that is the case there is also convection moreover diffusion. [10]

The resistance to transport of ions in electrolytes, which in HT-PEMFC are in the membranes, is called ohmic losses and results in a voltage drop and losses in the form of heat. The specific voltage that is needed to transport the charge with the current I can be seen as the ohmic resistance for ion transport. By measuring the current (I) between two probes in a material with a specific voltage (U) the ohmic resistance (R) can be calculated according to *equation 3.* [10]

$$R = U \times I \tag{3}$$

By dividing the length between two probes (L) with the cross-section area (A) and the ohmic resistance (R) from *equation 3* the specific ion conductivity, σ, can be calculated according to *equation 4*. [10]

$$\sigma = \frac{L}{A \times R} \tag{4}$$

To get a better representation of the resistance through a membrane, the area specific resistance (ASR) can be introduced. The ASR can be specified as the length that the charge needs to travel divided by the ionic conductivity of the membrane material (σ), see *equation 5*. [10]

$$ASR = \frac{L}{\sigma} \tag{5}$$

The proton conductivity of the electrolyte is essential for the performance of fuel cells. The proton transfer from the anode to the cathode is the rate determining step and can directly be linked with the current output, as can be read by *equation 3-5*. Likewise, the performance of a fuel cell can therefore be predicted if the resistance in the electrolyte can be determined. Finding an electrolyte with high proton conductivity is therefore one of the most important keys to receive higher efficiency in the future.

2.3.8 Membrane

Bagher Karimi et.al [20] summarised the most common ion conducting membranes in anhydrous conditions and these are Nafion®, polybenzimidazole (PBI), sulfonated polyether ether ketone (SPEEK), polysulfone (PS) and polyethersulfone (PES), polyimide (PI), chitosan (CS) and more recently poly (ionic liquid)s (PILs).

Nafion® is a copolymer using perfluoroethylene as the main chain and perfluoro vinyl ether as the side chain. Nafion® also contain sulfonic acid groups which is the component that gives Nafion® its ion conductivity. Nafion® usually shows excellent chemical and mechanical stability but the proton conductivity of Nafion® is determined by the hydration of the membrane with water. Therefore, in anhydrous applications Nafion® have had a decline in popularity and search for a new membrane has been made. Attempts to improve Nafion®s conductivity at anhydrous conditions have been made. This includes impregnation with deep eutectic solvents (DES), PA, IL amongst other. [20]

Poly ionic liquids (PILs) have come to attention in recent years as a promising alternative to the conventional membranes used today. PILs can be synthesised by many different methods such as crosslinking membranes, homopolymers, copolymers and block polymerisation. These processes lower the conductivity as the proton transferring spots is also the active sites for the polymerisation. [20] The conductivity range can vary a lot between different ionic liquids and temperatures. Kallem et.al [21] managed to achieve 330 mS/cm at 150℃ which makes it comparable to other membranes on the market today. The largest conductivity measured by PILs are, however, 1139 mS/cm with protic imidazolium based ILs at high temperatures (200℃) but the mechanical stability at these levels needs to be improved for it to be a viable alternative. [20]

Polyimide (PI) membranes has gotten some attention lately because of its thermal, mechanical and chemical durability and it can operate around 150℃ which allows working under anhydrous conditions. This contributes to countering the catalyst poisoning. However, in pristine PI membranes, the water is doing the main part of the proton conductivity with vehicle- and Grotthuss mechanism which makes the membrane have poor proton conductivity at higher temperatures and anhydrous conditions. To improve the conductivity the membrane can receive sulfonation or be doped with IL or PA. [20]

Sulfonated poly ether ether ketone (SPEEK) has gotten some attention for the application in PEMFC because of its good thermal and chemical stability as well as its flexibility and high conductivity when being sulfonated. The conductivity depends on the level of sulfonation of the membranes. There are several ways that have been tested to improve the properties of SPEEK including doping with IL, crosslinking polymers, blending with other polymers amongst other. SPEEK has shown conductivity as high as 100 mS/cm at anhydrous conditions and temperatures above 150℃. [20]

Chitosan (CS) has some prospects that have made it interesting for the use in PEM fuel cells. CS is biodegradable, cheap, biocompatible and easy to chemically modify. CS does, however, have low proton conductivity because of its high crystallinity so treatment like crosslinking, nano-composites and chemical treatment is needed when being used as a membrane in PEMFC. Even then, the proton conductivity of CS is lower than other alternatives being considered for HT-PEMFC. The highest conductivity that has been able to be measured is 80 mS/cm when having doped the membrane with acid and running at 150℃. [20] This is considerably lower than other membranes.

Polysulfone (PS) and Polyether sulfone (PES) are interesting alternatives to PA-PBI as both have great thermal and mechanical stability. PS and PES are cheap membranes with excellent properties and flexibility in use. They are easy to work with and are easy to dope with PA. PES and PS have shown conductivities up to 210 mS/cm at anhydrous conditions while being doped with PA. [20]

One of the most important membranes for HT-PEMFC today is the polybenzimidazole (PBI) membrane. The chemical structure of PBI can be seen in Figure 2. PBI has better mechanical and thermal stability at higher temperatures than Nafion® which is a necessity for membranes in HT-PEMFC. On its own, PBI does not have very high conductivity, but it is easy to dope PBI membranes with acids that greatly improve the proton conductivity. The most common acid to dope PBI with today is PA because of its stability, low vapor pressure and high intrinsic proton conductivity at higher temperatures. PA in PBI supports proton conductivity mainly through the Grotthuss mechanism and therefore the proton conductivity also depends upon the acid concentration in the membrane. It has been shown that PA-PBI can have a proton

conductivity up to 694 mS/cm under anhydrous conditions. [20] Aili et. al. [22] states that there can be a maximum of 10.2 PA molecules per repeating unit of PBI.

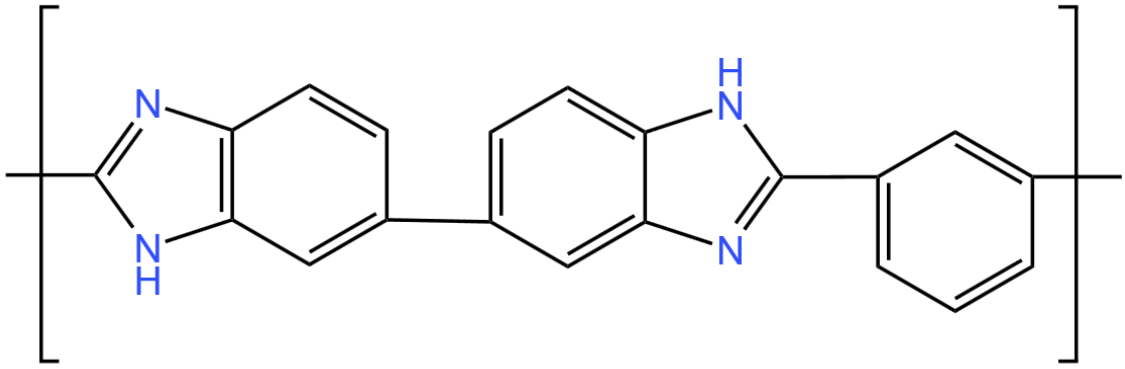

Figure 2. Repeating unit of Polybenzimidazole (PBI).

A problem with PA-PBI that has led to a search for a new membrane and electrolyte in HT-PEMFC is mainly the lowering of mechanical and thermal stability of the membrane at temperatures above 150°C. This becomes a problem since the temperatures HT-PEMFC is today often run at 160°C. There have been efforts to try to strengthen PBI by crosslinking the polymer, block co-polymerisation, synthesis of blend amongst other. [20] This is for creating a thinner membrane and by that lower the ASR of the membrane.

Table 2. A summary of membranes that have recieved some attention for the application in HT-PEMFC.

Membrane	Advantage	Disadvantage
Nafion®	Great mechanical and chemical strength	Water as charge carrier, making it undesirable at anhydrous conditions
Poly ionic liquids (PILs)	Good conductivity	Weak mechanical strength at higher temperatures
Polyimide (PI)	Good thermal-, mechanical- and chemical stability at anhydrous conditions	Water as charge carrier, making it undesirable at anhydrous conditions
Sulfonated poly ether ether ketone (SPEEK)	Flexible, good thermal and chemical stability. Good conductivity when sulfonated	Conductivity dependent on sulfonation level
Chitosan (CS)	Biodegradable, cheap and easy to modify	Low conductivity and chemical treatment needed
Polysulfone (PS)	Great thermal and mechanical stability, cheap and easy to work with	Conductivity dependent on phosphorylation
Polybenzimidazole (PBI)	Great mechanical and thermal stability at high temperatures	Conductivity dependent on phosphorylation

One of the most important properties for membranes in HT-PEMFC is durability. Degradation can lead to the membranes faulting in its mechanical, chemical or thermal durability and this can lead to fuel crossover. Fuel crossover is when hydrogen does not react with the catalyst and

instead moves through some holes or cracks in the membrane to the cathode side directly. This could lead to reaction directly between oxygen and hydrogen which would release all the energy in the form of heat instead of providing electricity. Membrane thinning is also a problem with membranes in HT-PEMFC that also could lead to fuel crossover. [16]

2.3.9 Ionic Liquids

Ionic liquids (IL) are liquids entirely composed out of ions that have a melting point under 100°C. They are often composed of large irregular organic cations combined with multiatom inorganic anions. The ions in an IL do not pack very well and there is a charge delocalisation which together lowers the melting point to under room temperature. This means that IL are in a liquid state at room temperature as well as usually having a very high crystalline temperature. This, together with having a very high ion conductivity, makes IL suitable for HT-PEMFC applications since it can stay in liquid state and do not form solid crystals over the entire temperature range that HT-PEMFC operates. [23]

One of the largest advantages of IL is the modifiability, exchanging one ion for another can change the properties of the IL. Properties such as melting point, viscosity, hydrophilicity/hydrophobicity, acidity/basisity, ion conductivity and more can be modified for the specific application. IL also have very low flammability and volatility. [16, 23]

High conductivity can be attributed to the high ion density which in turn also gives the liquid a density higher than water. IL can be divided into three different types, aprotic, protic and zwitterionic ILs. Aprotic IL are larger organic cations, such as pyridinium, that are mixed with smaller anions like bromine. Aprotic ILs do not have any active protons in their chemical structure which lead to that they cannot accept or donate hydrogen bonds. [16] Protic ionic liquids (PIL) are synthesised by a Brønsted acid and base which can act as a proton donor as well as a proton acceptor. That means that PIL have protons that can be exchanged between the ions. [17] Zwitterionic IL are when an IL is added to a surfactant system to modify its properties. [17] Aprotic IL are usually used in batteries while PIL most used in fuel cells. Zwitterionic are mostly used in IL based membranes. [17] The advantage of IL is that the ions can be chosen to give the desired properties. As PIL is the IL that is mainly used in fuel cells this report will mainly focus on these and will not go further into the other IL. PIL with nitrogen atoms and hydrogen atoms can form hydrogen bonds that enable Grotthuss transport mechanism. In Grotthuss mechanism, the ions get passed along ion acceptors and no movement is needed by the carriers. This can be compared with vehicle mechanism where the protons get transferred by that the transferring agent binds to the hydrogen and moves to the negatively charged point. Grotthuss mechanism is preffered in HT-PEMFC because there is no need for diffusion back of the charge carriers. [17] Otherwise, this would be important factor of the performance of the electrolyte.

Leakage of IL from the MEA in a HT-PEMFC is a problem in the application at higher temperatures of fuel cells. Alashkar et.al. [16] suggest future research into poly ILs that could possibly solve this problem.

Some ILs that have gotten some attention in the latest years are N,N-diethyl-Methyl Ammonium triflate ([dema][TfO]), 1-ethylimidazolium bis(trifluoromethylsulfonyl)imide [HEIm][TFSI], N,N-diethyl-N-methyl ammonium trifluoromethylsulfonyl amide [dema][TFSA] amongst other. [17, 23] Niu et.al [24] showed that [dema][TfO] could receive a conductivity high as 108.9 mS/cm at 250°C and [HEIm][TFSI] was noted with a conductivity of 54 mS/cm at 200°C which makes these very interesting in the application of HT-PEMFC. In Figure 3 the chemical structures of [dema][TfO] and [HEIm][TFSI] can be seen as well as

[FA][TFSI] which is a newly synthesised IL from Chalmers. According to Martinelli at Chalmers there is one pair of IL per repeating PBI unit in the membranes in this study.

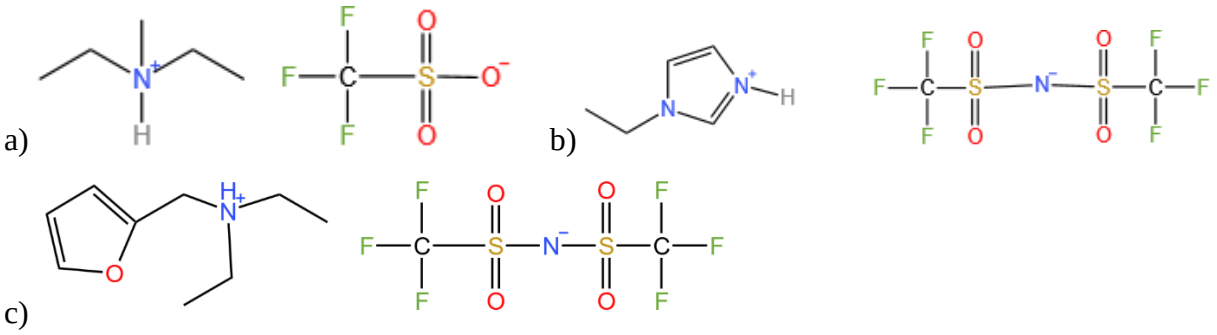

Figure 3. Chemical structures of the studied ionic liquids in this report. a) [dema][TfO], b) [HEIm][TFSI], c) [FA][TFSI].

2.4 Electrochemical characterisation

2.4.1 Polarisation curves

A plot of the cell voltage as a function of current density is called a polarisation curve. Polarisation curves can give information about the reaction that takes place at an electrode. This is because the current in the electrodes depend on the applied potential. However, when a current is running through an electrode there is deviation between the electrode's measured potential and the electrode's potential at equilibrium for the set temperature and reactant concentration. This difference is often referred to as the electrode being polarised. The overpotential, η, is the difference between the observed potential of a cell and the value at equilibrium state. The overpotential effect reduces the theoretical cell potential when the current is flowing. [10]

The polarisation curve can be divided into three different regions. The first is called activation polarisation. It is caused by the voltage overpotential needed to overcome the activation energy needed to get the reaction to take place. This has the largest effect at low current densities and is categorised by its sharp decline. In *Figure 4* the activation polarisation can be seen furthest to the left. The second region is the ohmic resistance polarisation. The ohmic polarisation is a collection of different resistances which includes the ionic resistance in the electrolyte, the resistance in the current collector as well as the electronic resistance in the active electrode material. All these resistances are directly proportional to the current applied which is why the polarisation curve is linear during the ohmic resistance polarisation region. At high current densities it is mostly concentration polarisation that dominates. This occurs when there are limitations to the mass transfer of reactants and products in the electrodes. To be able to remove products formed and to get the reactants to the active sites is critical in fuel cells and when the mass transfer is not sufficient this can be seen in the polarisation curve. In *Figure 4* the

concentration polarisation can be seen when the line departs from the linear path at high current densities.

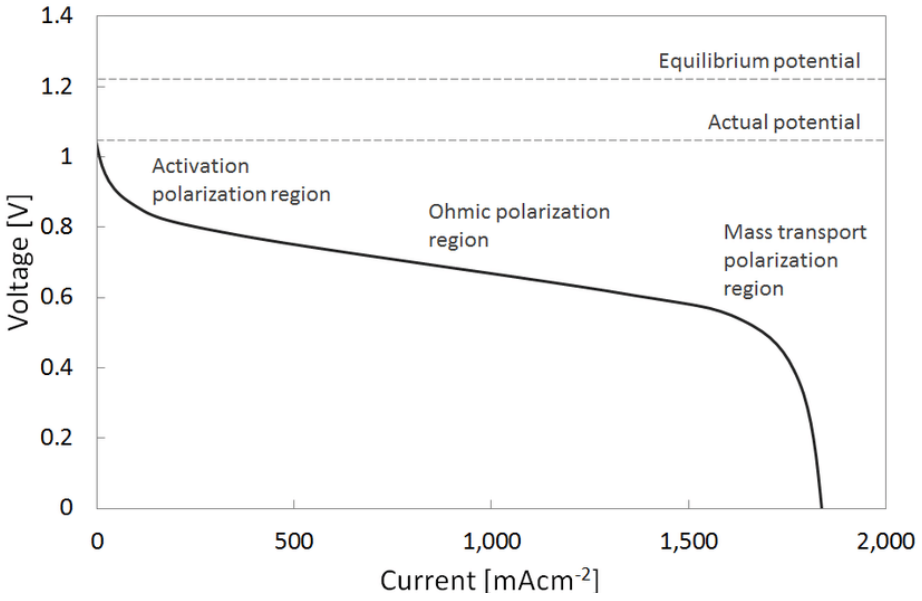

Figure 4. Theoretical appearance of a polarisation curve (or Potential-current curve)

When a cell is put under no current load it is called that the cell has open circuit voltage (OCV). The maximum chemical energy, E^0, of a cell can be calculated by subtracting the cathode potential by the anode potential. The OCV of HT-PEMFC operating with hydrogen and oxygen can then be calculated using Nernst equation which is depicted in *equation 7*.

$$E = E^0 + \frac{R \times T}{2 \times F} \ln\left(\frac{p_{H_2} \times p_{O_2}^{\frac{1}{2}}}{p_{H_2O}}\right) \tag{7}$$

Where E^0 is the half-cell potential, R is the universal gas constant, T is the temperature, F is Faraday's constant and P_i is the partial pressure of the gas i. Given that E^0 is 1.23V, see 2.3.4 and 2.3.5, the theoretical OCV can be calculated to be E = 1.215V at 160 °C. The actual potential is, however, substantially lower. In a well working fuel cell, the OCV usually is around 0.95V at 160 °C. The reason for this drastic difference between theoretical and measured OCV is not entirely understood. One theory is that side reactions can occur at lower current densities between H_2, O_2 and carbon impurities on the catalyst. Other reasons could be formation of H_2O_2 or the oxidisation of Pt catalyst. As been previously said, another reason for lower OCV could be fuel cross over. [25]

To get a polarisation curve the potential is reduced and the current is then measured. By plotting the voltage to the current divided by the working area you get a figure that should look something like *Figure 4*.

2.4.2 Electrochemical Impedance Spectroscopy

Electrochemical Impedance Spectroscopy (EIS) is a tool that helps to analyse different parts of a system. EIS can give information about the diffusion through a material, the reaction rate at an electrode and the ionic transfer rate in a membrane. This can be done by measuring the phase-shift of the sine wave to the applied current or potential, depending on which is being

measured and which is being controlled. [26, 27] For example, when applying high frequencies, the response is mainly due to fast processes, such as the ohmic resistance in the electrolyte, whilst lower frequencies give indication of mainly slow processes, such as reactions at an electrode or mass transport limitations. [26] The results can be visualised in different ways but the two most used are the Nyquist plot and the Bode plot. [26, 27] A Nyquist plot is the correlation between the real and imaginary parts of the impedance, Z. These are measured between given frequencies. The results of impedance plots are very complex and could be hard to interpret and a lot of different areas of the system can affect the curve. For complete analysis of EIS data for fuel cells there is a need for advanced physics-based models that are adjusted for each system studied. A widely accepted simplification is that the high frequency resistance (HFR), the point where the curve crosses the x-axis at the most left of the Nyquist plot, is attributed to the cell's ohmic resistance where the membrane resistance is the biggest contributor. [26] By knowing the membrane resistance you could then calculate the ion conductivity in the working condition of a cell with a specific membrane using equation 4. The cross-point at the most right at a Nyquist plot is used to find the low frequency resistance (LFR). The LFR is mostly contributed to by reaction kinetics and how they are affected by concentration resistances, such as slow diffusion and proton conductivity in the electrode. Since this project focuses on the membrane, the HFR is the most important to analyse. A Bode phase plot is when the degree of phase shifts is plotted against the frequency but will not be investigated in this report.

3 Materials and methods

3.1 Material

3.1.1 Electrode

The gas diffusion electrodes were prepared by depositing 60 wt% Pt/C powder to the carbon paper GDL by spraying from a formic acid-based ink. The amount of Pt/C powder was 0.037g and formic acid was 2.417g.

The Pt-loading of the electrodes used was 1.5 mg_{Pt}/cm^2. The specific electrodes used in the experiments were of 1.5 × 1.5 cm^2 area. The same type of electrode was used for the anode and cathode.

3.1.2 Membrane

The report is considering four different membranes. Three PBI membranes were casted together with three different IL. The IL were [dema][TfO], [HEIm][TFSI] and [FA][TFSI], see Figure 3. These membranes were casted in a petri dish. As a reference a PBI membrane doped with PA was used. The PBI membrane was doped by being placed in 85% PA for a long time (several weeks) to make sure they were fully doped. Pristine PBI membrane doped with 85% over a long time can maximally have 10.2 PA molecules per repeating PBI unit. [22] We can assume that this was the case because of the long time.

3.1.3 Charge carrier

This report used 4 different charge carriers in the membranes. Phosphoric acid 85% was obtained from DTU. [FA][TFSI] was synthesised at Chalmers and the [FA][TFSI]-PBI membrane were casted at Chalmers. [HEIm][TFSI] and [dema][TfO] were bought by Chalmer and [HEIm][TFSI]-PBI and [dema][TfO]-PBI casted at Chalmers.

3.1.4 Membrane Electrode Assembly

Membrane Electrode Assembly (MEA) were prepared by sandwiching the membrane between two electrodes held together with a Kapton® film. The Kapton® film (thickness: 50 μm) had a 1 cm^2 window in the middle. By having a specific size of the window and the reaction being fast enough, assures that the active reaction area was $1cm^2$.

3.2 Method

3.2.1 Spraying of Electrode

An important step in assembling the MEA is the spraying of the electrode with the catalyst solution. These experiments were made with a 60 wt% Pt/C powder. Before spraying, the catalyst powder was dispersed in formic acid. The performance of the electrode, and therefore also the fuel cell, depends partly on the catalyst loading of the electrode and an estimation of the average catalyst loading can be calculated according to *equation 6.*

$$Catalyst\ Loading = \left(W_{after\ spray} - W_{before\ spray}\right) \times wt\%_{\frac{Pt}{C}} \qquad (6)$$

where *W* was the weight of the carbon paper that was used as the gas diffusion layer before and after spraying the electrode solution. *A* was the area of the carbon paper. $Wt\%_{Pt/C}$ was the calculated weight percentage of the Pt/C powder. Catalyst loading usually has the unit mg/cm^2.

The carbon paper was heated on a plate heater at 150°C during the spraying. When the sprayer was ready, the catalyst solution was added to the sprayer and sprayed methodically onto the carbon paper. After the solvent evaporated, the carbon paper was rotated 90˚ before next spraying. The temperature was lowered continually over the spraying. The procedure of spraying and rotating continued until the solution in the sprayer was out. Then the carbon paper was weighed again.

3.2.2 Assembling of Fuel Cell

The IL-PBI membranes were in short supply, so the membranes were cut into 2×2 cm^2 squares at first. Later, the IL-PBI were cut into a quarter circle with a radius of 6.8 cm to get a bit larger area. The PA-PBI membranes were cut into pieces with larger areas, 5×5 cm^2, because there were more available of these. The membrane was placed inside a folded Kapton®-film. A gas diffusion electrode was placed on both sides of the membrane with the catalyst side towards the membrane. The MEA was then placed between two plastic sealing materials with 1×1 cm^2 windows in the middle. This is because the membrane should have an even pressure from the cell house. The plastic sealing materials and the MEA were then placed in the fuel cell house where the current collectors have gas channels too evenly spread the gas over the GDL. The fuel cell house was then closed. The bolts were tightened to a sealing force of 2 Nm, stepwise and diagonally to ensure an even pressure across the cell.

For the IL-PBI membranes all tests were done in three ways; without addition of any dopant, doped with 1 drop of PA on each side of the membrane and doped with 1 drop of corresponding IL on each side of the membrane.

3.2.3 Membrane ionic conductivity test

To test the proton conductivity of the different electrolytes an in-plane ionic conductivity test was conducted. Four electrodes were contacted with the membrane and a 1-2 kHz symmetric square wave current was applied between the outer electrodes using a pulse generator. A 1cm wide and 5cm long strip of membrane was placed on the holder, seen in Figure 5, where a current is passing through the membrane made by the pulse generator. The voltage drops between the two inner probes, with 1cm between, was measured using an oscilloscope. The resistance R was calculated using ohms law, and the conductivity was calculated based on the sample dimensions and the recorded resistance. In *equation 5* the *L* is the length between these probes, *A* is the cross area which is the width of the strip times the thickness.

Figure 5. Set up for the measuring of proton conductivity.

To get the temperature dependency for the ionic conductivity of the membranes the membrane holder was placed in an oven where the temperature was controlled manually. Temperature tested were 20℃, 60℃, 80℃, 100℃, 120℃, 140℃, 160℃, 180℃.

In an oscilloscope you get a box shape curve if the electrons can be polarised, inducing a current of protons in the membrane, in the frequency given. If not, the curve can receive different shapes that are not box shaped. This could mean that the material does not conduct sufficiently well. In the conductivity tests the potential and current can be read from the oscilloscope by placing the measurer and reference line at the top and bottom respectively at the box shaped curve. If there are no box shapes, the potential and current collected from the probes are not accurate.

For the IL-PBI membranes a symmetric square wave current could not be generated, and accurate reading of current and voltage drop were therefore not possible. The decision to test if it would work with a drop of PA was made. Lastly, a drop of corresponding IL on the membrane was also tested.

One drop of PA weighs 0.038 g and PA has a molar mass of 97.994 g/mol. This means that $3.88 * 10^{-4}$ mol PA was added to the membranes. Given from Chalmers was that there was a 1:1 mol ratio between IL and PBI in the IL-PBI membranes. The molar mass of each IL was 237.24, 377.3 and 434 g/mol for [dema][TfO], [HEIm][TFSI] and [FA][TFSI] respectively. PBI has a molar weight of 308 g/mol. By dividing molar masses of the IL and PBI you get how much (g) IL per repeating PBI unit. Dividing the weight of the membrane with the weighed molar masses you get the number of repeating PBI units. Dividing the mol of PA with the mol of PBI you get amount of PA per repeating PBI unit in the IL-PBI membrane. Values of the calculations can be seen in Table 3.

Table 3. Table of calculations of amount of PA per repeating PBI unit.

Membrane	Molar mass of the IL [g/mol]	IL:PBI weight ratio [g_{IL}/g_{PBI}]	Mol PBI [n_{PBI}]	Mol PA per repeating unit PBI
[dema][TfO]-PBI	237.2	0.77	$4.93 \cdot 10^{-5}$	7.867
[HEIm][TFSI]-PBI	377.3	1.23	$3.635 \cdot 10^{-5}$	10.67
[FA][TFSI]-PBI	434.0	1.41	$3.05 \cdot 10^{-5}$	12.73
PA-PBI	N/A	N/A	N/A	10.2

3.2.4 Characterisation techniques

The single cell tests were done in a rig at DTU. Hydrogen and air were provided and assembled in counter flow. Heater and temperature control were also connected to the cell. Potential and current measures were connected last. Heater was turned on to 160℃.

All single cell tests were run for over 3 days (>70h) to ensure steady state. PA-PBI was activated before doing upcoming tests by running at 0.1V load. Due to instable performance for the IL-PBI membranes, these were run at OCV conditions instead.

When the single cell tests had been active for the minimum time, a polarisation curve test was run to give an indication of the performance. Both OCV and final current density were noticed as well as saving data for the polarisation curve. More on how polarisation curve tests were

done in chapter 3.2.4. After the polarisation curve, EIS was done and more about this in chapter 3.2.5. Then the temperature was lowered to 140℃, 120℃ and 80℃. EIS tests were run on every temperature. The single cell tests used 100 mL/s pure hydrogen gas as fuel on anode side and 400 mL/s air on cathode side.

3.2.5 Polarisation curve

Polarisation curves were done by using potentiostats from VersaStat. For a reminder about the theory behind polarisation curves, see chapter 3.4.1. First, the system ran at OCV conditions for 30 seconds. Then the potential was swept from OCV to the end point at 0.15V. The system measured 1000 points between the OCV and the set end voltage point with a scan rate of 0.002 V/seconds. Polarisation curves included in this study were done at 160℃.

3.2.6 Electrochemical Impedance Spectroscopy

EIS measurements were done by using potentiostats from VersaStat. Theory about EIS can be read in chapter 3.4.2. Firstly, the program ran 30 seconds of OCV conditions. Thereafter a potentiostatic EIS measurement was done at OCV conditions followed by galvanostatic measurements done at 0.2A and 1.0A. The frequency was scanned from 100000 Hz to 1 Hz with an amplitude of 50 mA. At the membranes that did not show a performance of 0.2 A and higher at the polarisation curves were not run at 0.2A or 1.0A. EIS measurements were done at 160℃, 140℃, 120℃ and 80℃ in order.

4 Results and Discussion

4.1 Methodology validation

To ensure that the results were going to be valid and could be trusted, validation of the methodology was needed. This was done by doing the experiments with a well-tested membrane, namely PA-PBI.

4.1.1 Conductivity tests

Ion conductivity is a key function of polymer electrolyte membranes. Testing if a material has good conductivity is therefore important to find a material that is a good fit for HT-PEMFC. There are, however, many other characteristics that a material need (such as good contact with electrode, high part Grotthuss mechanism, mechanical and chemical strength amongst other) so just because a material does well in a conductivity test does not mean it is a good fit for HT-PEMFC. The conductivity can also vary depending on temperature. By doing the test at different temperatures you could get an idea at what temperatures a material conducts the best which is useful in the design of a fuel cell.

To have a reference when doing the IL-PBI membranes, the first tests were done with PBI membranes that were doped with PA (10.2 PA per repeating PBI unit). By placing the membranes in 85% PA for a long enough time that the membrane is fully doped with the PA this should give a good reference that is close to the state of the art of HT-PEMFC membranes today. Figure 6 shows the conductivity depending on the temperature for PA-PBI membranes at three different tests using different pieces of membrane every time. The potential and current were looked at with three different frequencies at every temperature, therefore the three dots per temperature and colour. The conductivity was calculated using *equation 3-5*. Optimally, the dots should not differ but there is some human error and small adjustments could have a substantial impact on the results.

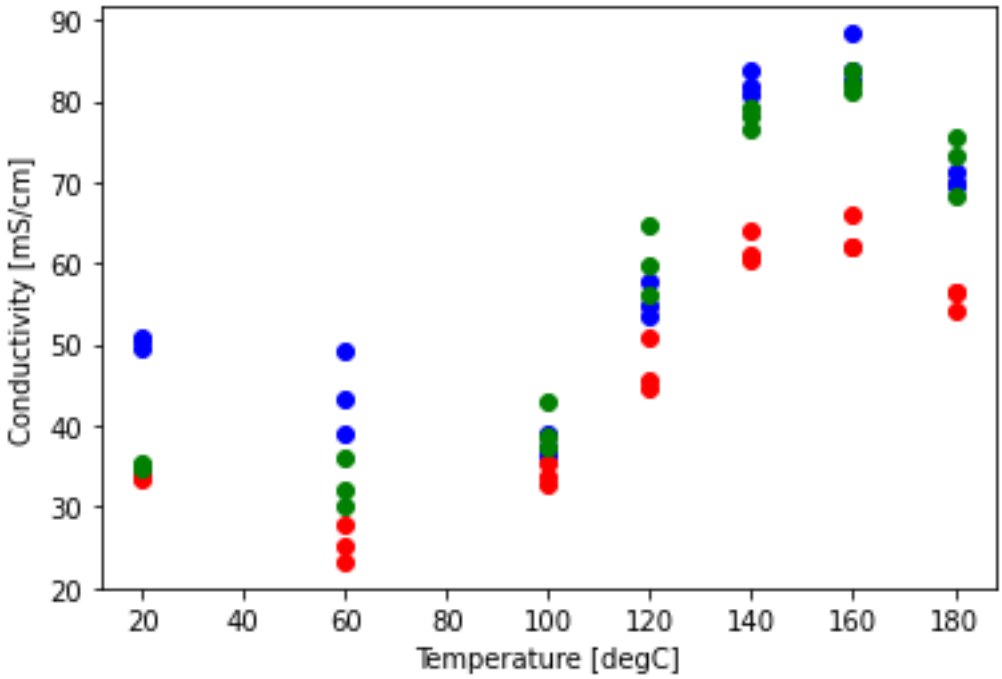

Figure 6. Conductivity tests of PA-PBI membranes depending on temperature. The different colours correspond to the samples evaluated. Three different frequencies were looked at per temperature, as shown by three dots per temperature.

The difference in conductivity at lower temperatures could be attributed to different humidity in the room where the experiments took place as the results become much more stable at temperatures over the boiling point of water. We can therefore assume that there is negligible amount of water in the membranes over 100°C. The results from the PA-PBI conductivity tests (a conductivity of >80mS/cm) correspond well with what can be found in literature [28, 29] as well as that the different tests follow a similar pattern, verifying the measurement methodology. The machine was controlled manually and small errors in the reading of the result can have some impact which can account for the differences of the blue and green test in Figure 6. The red test differs from the others substantially at higher temperatures. The membrane should have the same doping as the other two tests so why it has a lower conductivity is unclear. The tests were dabbed with a paper cloth to remove access PA so this could have had an impact on the result. This could affect the conductivity since the conductivity depend on the level of doping.

4.1.2 Polarisation curve

Polarisation curves were done by varying the potential and measuring the current and dividing it by the active area of the electrode to get the current density. Firstly, PA-PBI membranes were tested several times to try to get a method of assembling the cell that gave results that were comparable to state-of-the-art cells. First few experiments the fuel cell had no potential at OCV conditions, meaning that no voltage nor current could be measured from the cell. A working cell should have an OCV over 0.75V and if there is none this could be caused by different factors. The most likely reason here was found to be fuel leakage from anode to cathode. This could be due to a membrane with have imperfections, like small holes, or that the fuel in some other way can pass by the membrane and mix with the gas on the other side. This is why a methodology in setting up the cells was needed.

When the cells became more stable and gave reproducible results the polarisation curves of the reference membrane, PA-PBI, was measured. Figure 9 shows the results of three different cell tests using PA-PBI as the membrane.

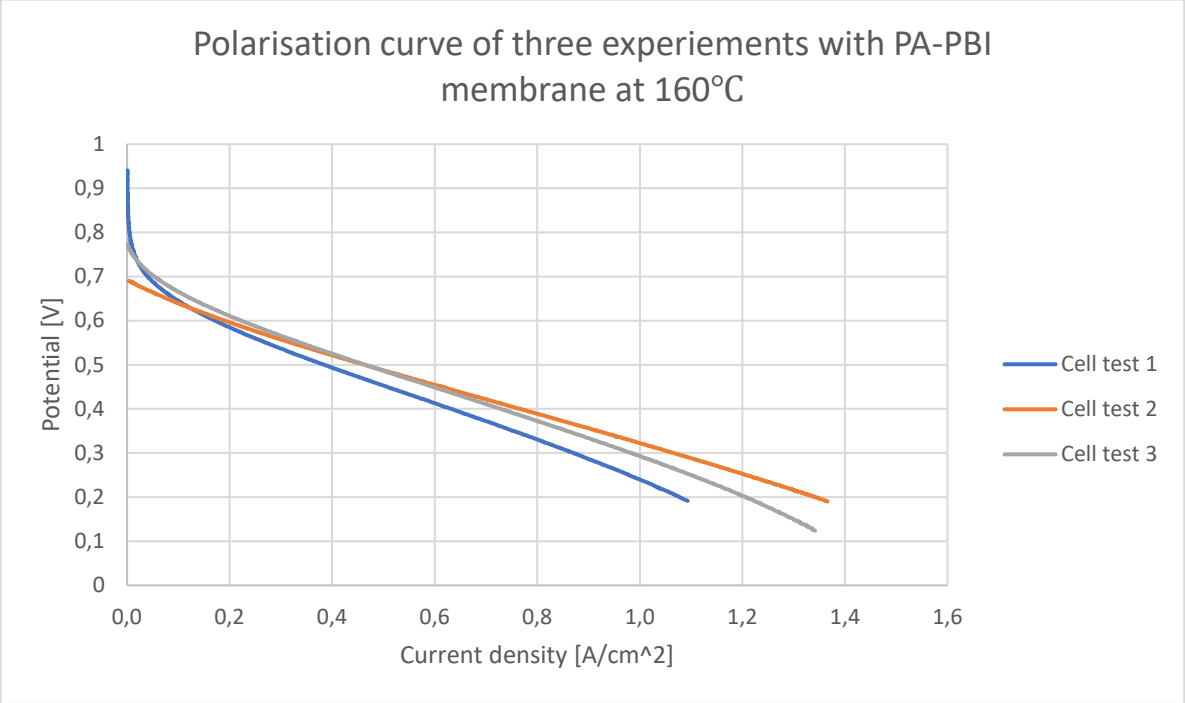

Figure 7. Polarisation curve of three different single cell tests using PA-PBI membranes.

From Figure 7 it can be seen that the OCV, which is at zero current load, where the curves cross the y-axis, is dissimilar. Cell test 1 had the highest OCV, indicating the best put together cell. Cell test 2 had an OCV below 0.7V but has the lowest decline which suggests that this run had the lowest resistance. Otherwise, the graph shows that the cell tests have similar results and correspond well to the literature. [30] Therefore, the methodology is good and cell tests for the IL-PBI membranes can be done and the results can be compared to the reference PA-PBI membrane.

4.2 IL-PBI membrane results

4.2.1 Conductivity

When trying to do the same test for the IL-PBI membranes from Chalmers, symmetric square wave current could not be obtained which implies that the materials cannot maintain the flow of ions during the pulses. This is a sign that materials have high resistance and therefore very low conductivity by themselves. To test if this was the case, one drop of PA (see Table 3) was allowed to sink into the membranes when the membrane still was in the rigg. When no extra PA could be seen on the membranes the membranes were tested again. Now a potential and current could be collected from the oscilloscope, even though the current pulses were not fully symmetric, as is desired. The results can be seen in Figure 8.

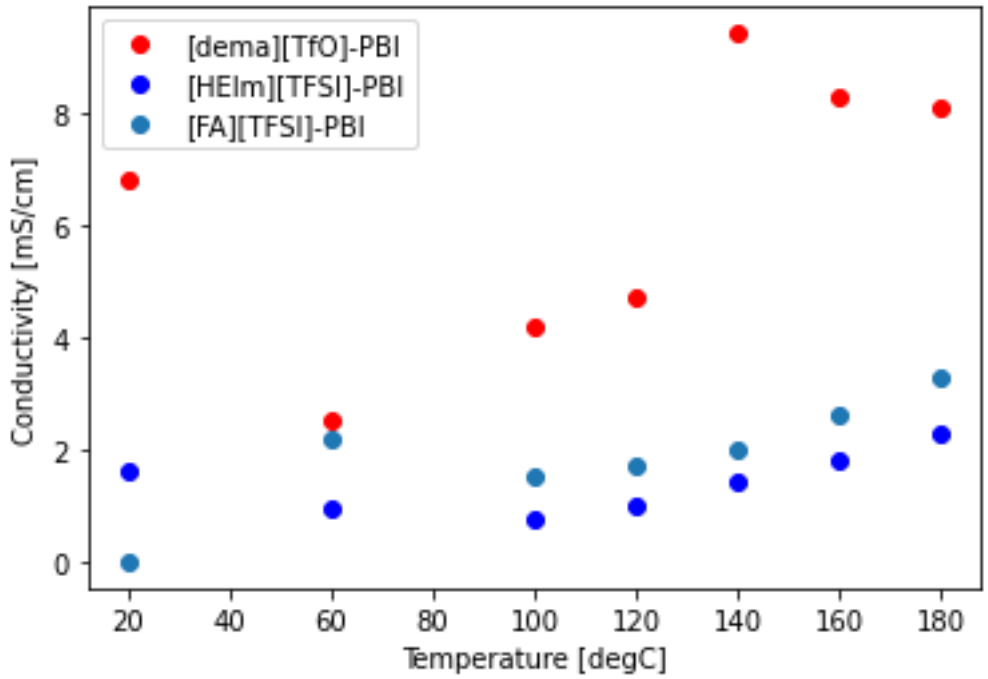

Figure 8. Conductivity of all the IL-PBI membranes with a drop of PA, depending on the temperature.

The membranes do not have the same stability as the PA-PBI membranes. Also, the conductivity of the IL-PBI membranes have very poor conductivity even with a drop of PA. Figure 9 shows the IL-PBI membrane's conductivity in the same graph as a PA-PBI membrane on a logarithmic scale.

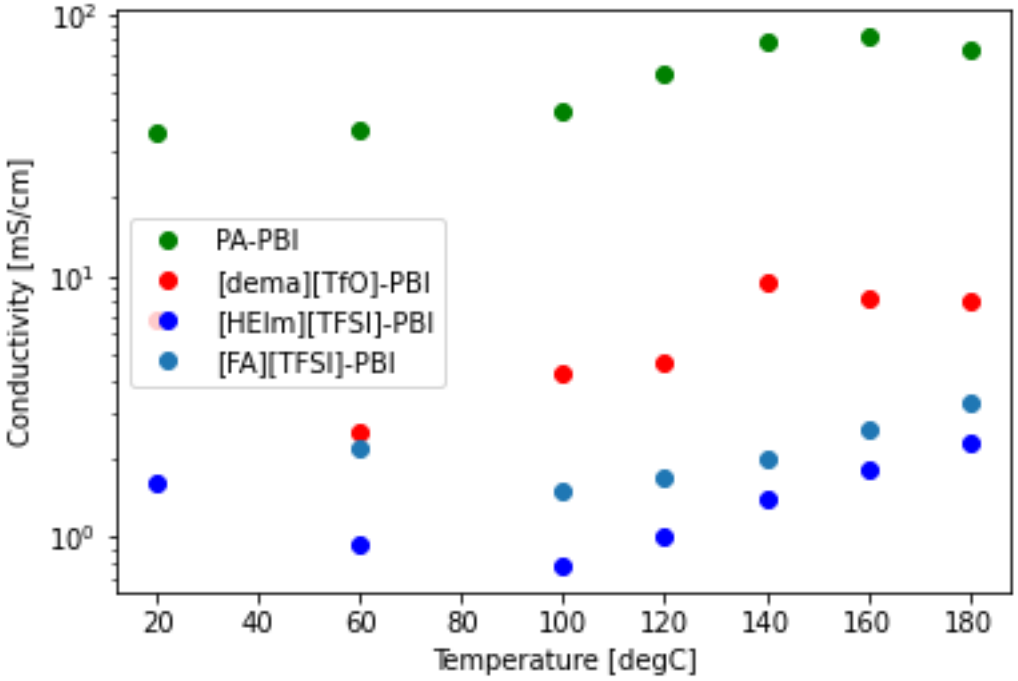

Figure 9. A graph showing the conductivity on a logarithmic scale depending on temperature of all the membranes included in the study.

Figure 9 shows some clear results. None of the PA doped IL-PBI membranes perform as well as PA-PBI membrane. [HEIm][TFSI]-PBI and [FA][TFSI]-PBI had similar curves except somewhat shifted. This could have something to do with that they both have the same corresponding ion, [TFSI]. [dema][TfO]-PBI had the best in-plane conductivity of the IL-PBI membranes according to these tests. The results of the calculations can be seen in Table 4. The resistance in Table 4 has been calculated using *equation 3*, using the measured potential and current at the temperature. The conductivity, in turn, uses that resistance for *equation 4*. With the conductivity you can then estimate the area specific resistance, ASR, for the different membranes with *equation 5*.

Table 4. A table showing the area specific resistance of the different membranes studied at 160°C. The IL-PBI membranes have been doped with 1 drop of PA.

Membrane	Resistance at 160°C [Ω]	Conductivity at 160°C [mS/cm]	Membrane thickness [cm]	Estimated ASR* [Ωcm^2]
PA-PBI	1215	82.3	0.01	0.12
[dema][TfO]-PBI	12048	8.3	0.01	1.2
[HEIm][TFSI]-PBI	84175	1.8	0.0066	3.7
[FA][TFSI]-PBI	33921	2.6	0.011	4.2

* Assuming that the membrane is isotropic and that the through-plane conductivity equals the in-plane conductivity.

It is clear that the in-plane conductivity for the PA doped IL-PBI membranes is very low, a factor 10 lower, then the PA doped PBI membrane. This results in a higher ASR which should make these membranes a worse fit for use in HT-PEMFC. [HEIm][TFSI]-PBI and [FA][TFSI]-PBI have higher ASR than [dema][TfO]-PBI and PA-PBI.

Experiments were made by Chalmers on two of the membranes included in this study, [HEIm][TFSI]-PBI and [FA][TFSI]-PBI. The result received are the in-plane conductivity and without addition of PA. The results can be seen in Table 5.

Table 5. Data received from experiments done on [HEIm][TFSI]-PBI and [FA][TFSI]-PBI done by Chalmers.

	[HEIm][TFSI]-PBI		[FA][TFSI]-PBI	
T (°C)	log(σ_{DC} [S/cm])	σ_{DC} [S/cm]	log(σ_{DC} [S/cm])	σ_{DC} [S/cm]
25	-7.1493	$7.09 * 10^{-8}$	No stable plateau	
40	-6.53013	$2.95 * 10^{-8}$		
50	-6.22371	$5.97 * 10^{-7}$		
60	-5.97798	$1.05 * 10^{-6}$	-9.5302	$2.95 * 10^{-10}$
70	-5.76926	$1.70 * 10^{-6}$	-8.97982	$1.05 * 10^{-9}$
80	-5.58099	$2.63 * 10^{-6}$	-8.52665	$2.97 * 10^{-9}$
90	Tests not done		-8.18032	$6.60 * 10^{-9}$
100			-7.82435	$1.50 * 10^{-8}$
110			-7.45097	$3.54 * 10^{-8}$
120			-7.06998	$8.51 * 10^{-8}$

Table 5 shows that the conductivity of the membranes is very low. This validates the results of the experiments done in this report. When the conductivity is less than a nS/cm, which some of the results show in Table 5, the material could almost be seen as an isolator which is not desired in a conducting membrane. A similar result could probably be expected from the report when using dry IL-PBI membranes, but the equipment used could not read results that low.

Figure 10 shows an Arrhenius plot of the membranes tested.

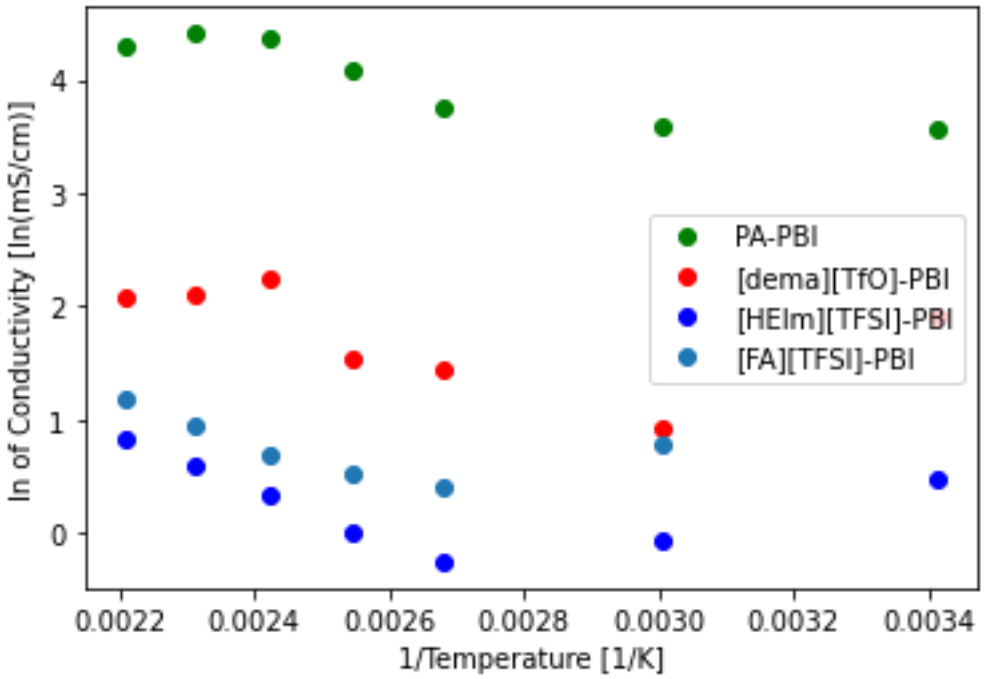

Figure 10. Figure shows an Arrhenius plot for the membranes.

Arrhenius plots can be used to predict activation energy if a linear curve is obtained. Figure 10 has no linear curves so no such energy can be estimated from this test.

All the membrane's conductivity improves with increasing temperature, at least to a point. PA-PBIs conductivity starts to fall off above 160℃ and this is probably attributed to that PA starts to evaporate at 180℃.

4.2.2 Polarisation curves

Every cell test was run several times to verify the continuity of the cells and the results followed the same curve, just like in Figure 7. Only one iteration per cell test is used in the graph, however, to make the graph more readable.

When running the IL-PBI membranes in single cell tests, without adding PA, there was no potential nor current obtained. It is probable that the membranes did not have very good contact with the electrodes and therefore no potential difference could be obtained. When there seemed like nothing was happening in the cell after an hour, the cell was taken apart and a drop of PA (0.038g) was added to both side of the membrane. PA was added for two reasons: 1) to give a better connection between electrode and the membrane. It was thought that perhaps the cell did not work since there were no bridge between the electrode, producing the ions, and membrane. 2) to be the ion carrier in the membrane. It is probable that the PA added also sunk into the membrane. When the PA had been added and put back into the testing rig the system showed an OCV. Probably, the PA added had the biggest effect on the connection between the membrane and the electrode because the big difference in OCV before and after. To be able to receive any results and to be able to compare, all IL-PBI membrane tests were doped with 1 drop of PA.

In Figure 11 all the cell tests of the PA doped IL-PBI membranes are included and it can be seen that the performance of the IL-PBI membranes are far below the performance of the PA-PBI membrane.

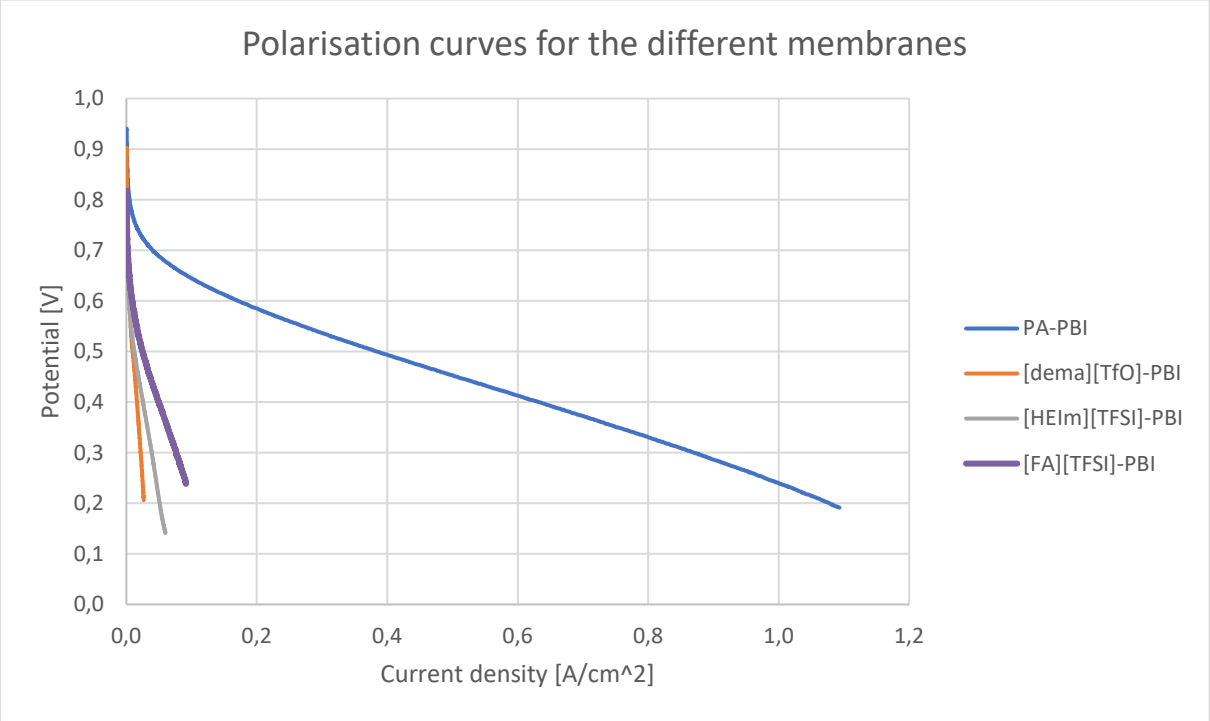

Figure 11. A graph showing polarisation curves of the different membranes in the same plot. The temperature was 160°C for all tests and 1 drop of PA was added to each side of all three IL-PBI membranes.

Worth mentioning is that the quality of the cells varies according to Figure 11. The OCV goes from about 0.75V for [HEIm][TFSI]-PBI to PA-PBI that has an OCV of about 0.95V. The reason is probably that the cells with lower OCV have some fuel leakage. The IL-PBI membranes were in short supply and smaller bits of membranes were needed to be cut out to be able to do all the tests intended in the study. There was a lot of PA-PBI available and larger membranes were used in these experiments. This should only affect the OCV since the electrode and window in the Kapton®-film was set to the same size for all experiments. Fuel leakage could also occur if there is a hole in the membrane. A lower OCV in a cell test could therefore be attributed to a defect in the membrane, gas getting to the other side without passing the membrane. It could also be that the membranes were thinner at specific spots which could allow gas through more easily. The membranes were made by solution casting in petri dishes and this methodology can affect membrane morphology. Furthermore, the membranes are experimental and not fully characterized, it is therefore difficult to predict how sensitive these membranes are to previous handling. The membranes were also slightly visually different where various parts were oblique and other opaque. When measuring the thickness of the membranes it varied from 60 µm to 140 µm. Especially, at some of the opaque parts the membranes were substantially thinner than other parts of the membranes and could perhaps be more permeable for hydrogen. This would result in lower OCV. The membranes also have unknown porosity and determining the porosity could be a topic for further studies.

By looking at the PA-PBI curve in Figure 11 it can be seen that the voltage was slightly lower than 0.6V when at a current density of 0.2A/cm^2, which is a common point of comparison. None of the IL-PBI even gets to that amount of current, at 0.6V they have a current density of

5.7, 4.0 and 9.3 mA/cm^2 for [dema]TfO]-PBI, [HEIm][TFSI]-PBI and [FA][TFSI]-PBI respectively. It is hard to see clearly the differences of the IL-PBI membranes in Figure 11 because of their poor performance. To get a better look at the performance of the IL-PBI membranes the PA-PBI membrane was taken out and the result was Figure 12.

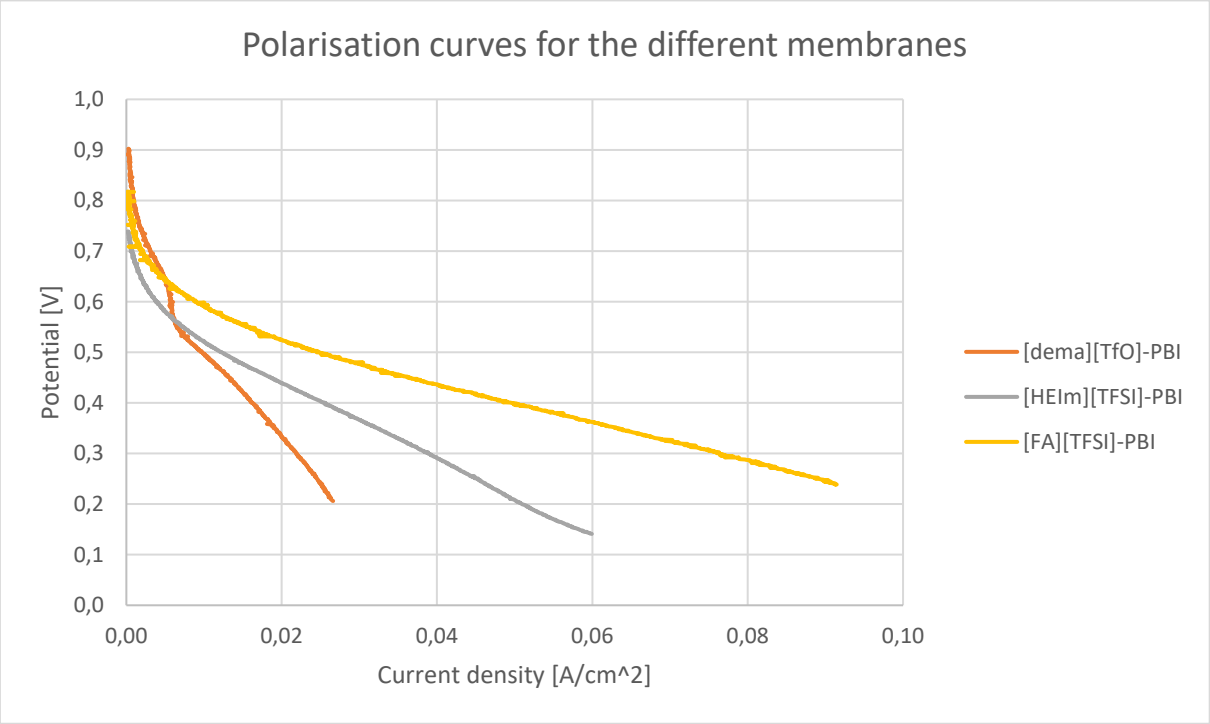

Figure 12. A graph showing polarisation curves of the IL-PBI membranes at 160℃ that have been doped with 1 drop of PA on each side of the membrane.

It is clear in Figure 12 that [FA][TFSI]-PBI has a better performance than the other two IL-PBI membranes. This could perhaps be attributed to that [FA][TFSI]-PBI has an higher PA per repeating PBI unit, since PA is a good conductor and a higher level of doping usually means higher conductivity. This theory is strengthened with that [HEIm][TFSI]-PBI has the second to best performance and has the second to highest PA per repeating PBI unit. It can also be seen that the curves contain a lot of bumps which could indicate that the cells are unstable. The [HEIm][TFSI]-PBI membrane had a smoother line, suggesting a slightly more stable cell but still not as stable as PA-PBI. The [dema][TfO]-PBI membrane had very little increase of current density between 0.65V and 0.55V and it is unclear why.

To identify a possible reason for the poor performance of the PA doped IL-PBI membranes the total resistance in the operating cell can be compared to the estimated ASR based on the results from the conductivity data in Table 4. When looking at Figure 11 and Figure 12, all the curves are linear between 0.5V and 0.3V. The total resistance was therefore calculated as the quotient between the voltage change and current density change between these points. The results can be seen in

Table 6.

Table 6. The ohmic resistance calculated from the polarisation curves compared to the ASR calculated from the conductivity tests.

Membrane	Total resistance from polarisation curve [Ωcm^2]	Estimated ASR from conductivity tests [Ωcm^2]
PA-PBI	0.41	0.12
[dema][TfO]-PBI	16.6	1.2
[HEIm][TFSI]-PBI	7.5	3.7
[FA][TFSI]-PBI	3.9	4.2

The trend in

Table 6 is that the membranes have similar resistances in both cases. The total resistance, however, include more factors than just the membrane resistance that is covered in the ASR, for example the reaction kinetics and mass transport resistance is included in the total resistance. We can therefore expect the total resistance calculated from the polarisation curves to be higher, which we see in all cases except for [FA][TFSI]-PBI, and this is discussed more in connection to the EIS measurements below.

There are some uncertainties that are hard to rule out in cell tests. The fuel leakage is one source of error that has been discussed before. Another source of error could be the doping of the IL-PBI membranes. Since the cell test of the IL-PBI membranes showed little to no potential nor current when not adding some PA between the electrode and membrane it is hard to say how much the membranes conducted protons and how was contributed to the added PA. The results in these polarisation curves, and later impedance measurements, should be seen as PA doped IL-PBI membrane results. To test the significance of the PA, doping the IL-PBI membranes with corresponding IL were done and very poor performance could be seen, see Figure 13.

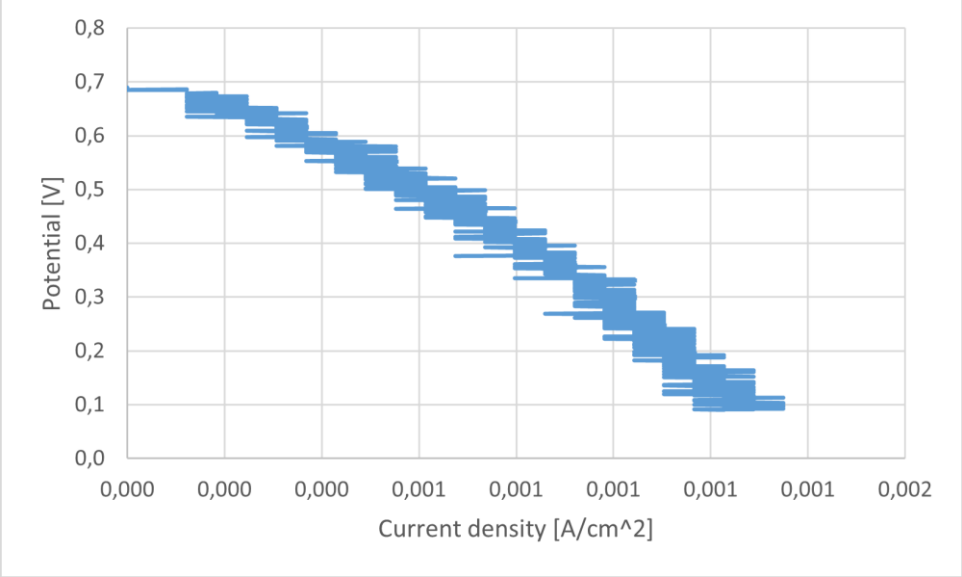

Figure 13. Polarisation curve of [dema][TfO]-PBI membrane with a drop of [dema][TfO] on both sides of the membrane.

Because of that both no PA doping and doping with IL gave very poor performances it can be concluded that the PA added is doing most of the conducting in IL-PBI membrane tests. Calculating the total resistance from Figure 13 you get 544 Ωcm^2 which is substantially higher than the total resistance of PA doped IL-PBI membranes. The IL does give a bridge between electrode and membrane, however, which is an important find.

No experiments were done to measure the actual amount of PA in these membranes, only estimations, but this could be of interest in the future if the possibility of PA doped IL-PBI membranes is of interest. This does not, however, solve the case of finding a substitution to PA doped membranes in HT-PEMFC.

4.2.3 Impedance measurements

The impedance tests were run using a potentiostat from VersaStat and the software VersaStudio. All tests presented in this chapter were run with 1 drop of PA on each side of the membranes since no OCV could be seen when running without it. The tests were run with 5 iterations in the beginning to verify that the program and system were stable. All the iterations gave similar results, see appendix. Moreover, every membrane was run twice to catch any malfunctioning systems. In the graphs only one iteration and from one test is presented to simplify the understanding and make the results clearer. Figure 14 shows the Nyquist plots of the impedance measurements of the membranes at different temperatures.

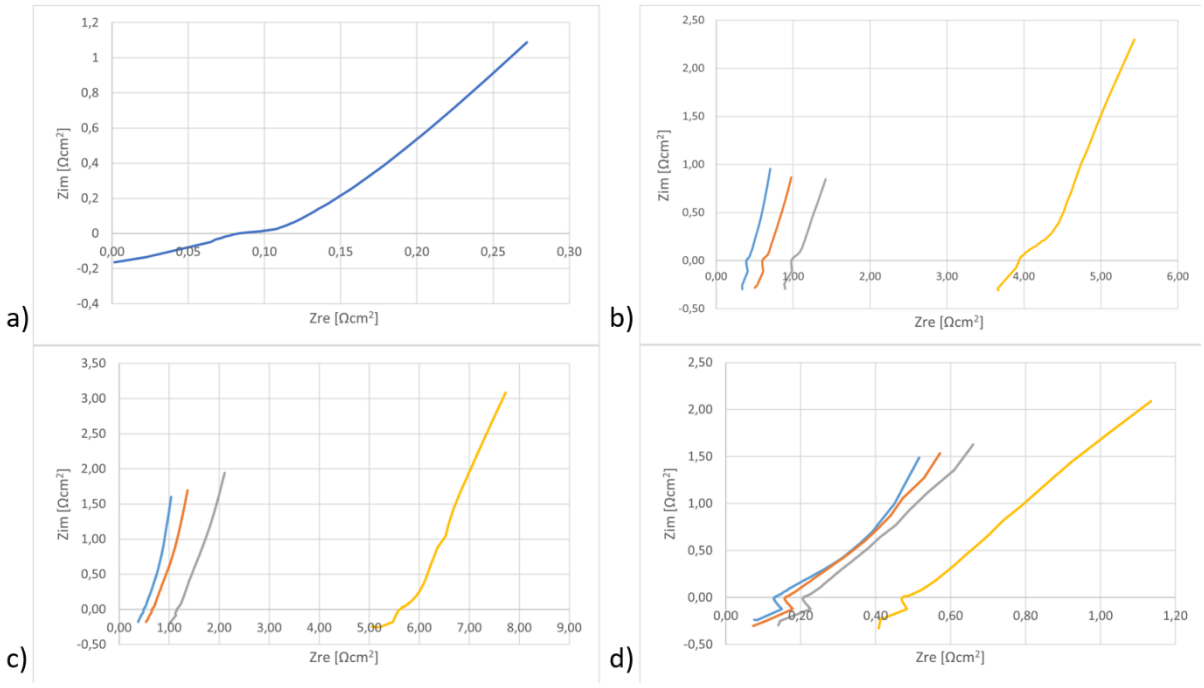

Figure 14. Graphs showing the impedance measurements in Nyquist plots at OCV where the graphs corresponding to a) PA-PBI, b) [dema][TfO]-PBI, c) [HEIm][TFSI]-PBI and d) [FA][TFSI]-PBI at OCV conditions. Blue, orange, gray and yellow lines correspond to 160°C, 140°C, 120°C and 80°C respectively.

From Figure 14 a clear temperature dependency can be seen. As temperature increases the high frequency intercept is lower on the x-axis for all membranes. This means that the resistance of the membrane gets lower as the temperature rises, which is in line with the results from the conductivity studies. For PA-PBI EIS was only measured at 160°C because of a miss in the planning. The graphs show that the resistance in the membranes is lowest at 160°C for all

membranes. To compare the membranes to each other, in Figure 15 only the impedance measurements from 160℃ have been plotted.

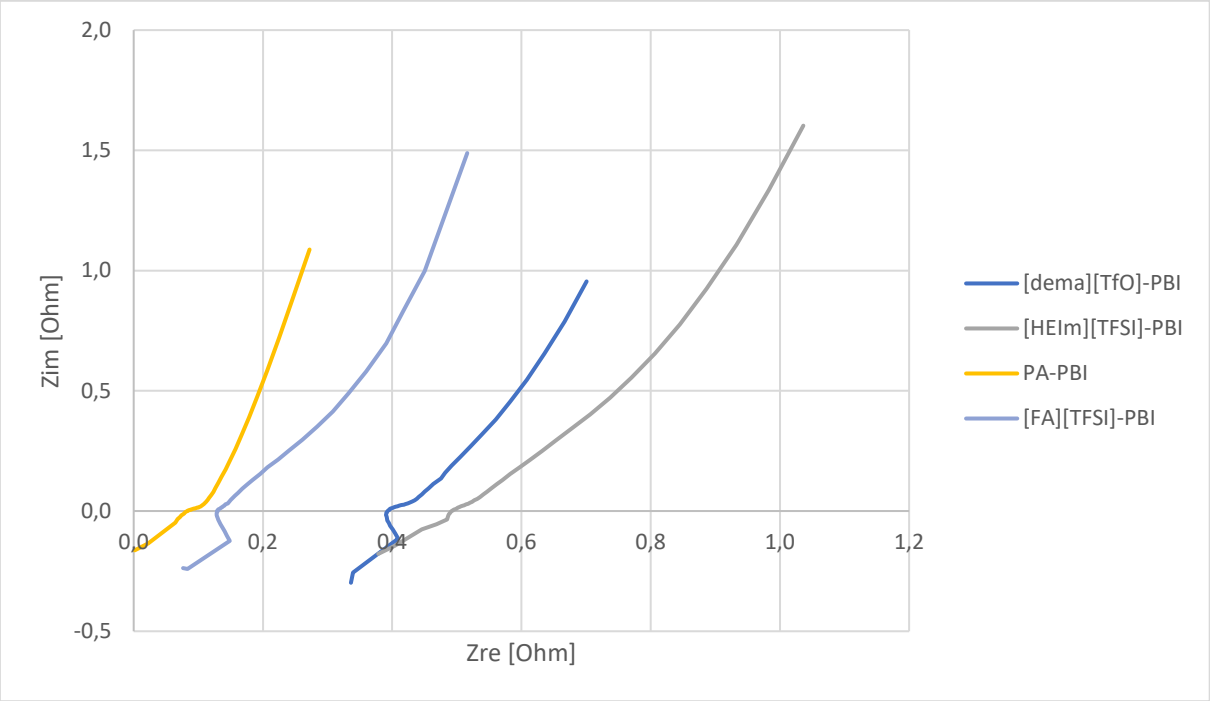

Figure 15. A graph showing a Nyquist plot of all the membranes at OCV conditions and 160℃. The high frequency intercept is where the curve crosses the x-axis.

The figure gives a clear indication that PA-PBI has the lowest resistance followed by [FA][TFSI]-PBI, [dema][TfO]-PBI and lastly, [HEIm][TFSI]-PBI. Table 7 shows the through-plane conductivity, data used to calculate it (high frequency intercept and membrane thickness) and the in-plane conductivity measured in the conductivity test for comparison. The membrane thickness was measured at 5 different spots on the membrane and a mean value was taken. When the thickness of the membranes was measured [HEIm][TFSI]-PBI was the thinnest. The other three were similar in thickness. The through-plane conductivity was calculated using *equation 5* where L is the membrane thickness, R is the measured resistance and A is the electrode area exposed to the membrane which was 1 cm^2.

Table 7. The high frequency intercept on the real impedance measurements at 160℃. The through-plane conductivity and in-plane conductivity has been calculated and collected.

Membrane	High frequency intercept [Ω]	Membrane thickness [cm]	Conductivity through-plane [mS/cm]	Conductivity in-plane [mS/cm]
PA-PBI	0.083	0.010	120	82.3
[dema][TfO]-PBI	0.39	0.010	26	8.3
[HEIm][TFSI]-PBI	0.49	0.0066	13	1.8
[FA][TFSI]-PBI	0.13	0.011	84.6	2.6

What stands out when looking at the result is the good through-plane conductivity of the [FA][TFSI]-PBI membrane as it is substantially higher than the other IL-PBI membranes. It is however still lower than PA-PBI. That the [FA][TFSI]-PBI membrane also have a lot higher through-plane conductivity than in-plane could mean that [FA][TFSI]-PBI membrane have good channels where ions can pass through when going through the plane but is more rigid in-plane. Perhaps that the polymer has aligned itself in one way instead of creating a grid. PA-PBI is the best membrane when looking at the Nyquist plots. The difference could also be because of the uncontrolled addition of the PA. This higher conductivity measures in an operating single cell can explain the reverse behaviour seen for this membrane in

Table 6. Where the total cell resistance was lower than ASR calculated from in-plane measurements. The membranes could have been doped with different amounts that probably would affect the results, if this was the case.

It was clear that when doping the IL-PBI membranes with PA the results improved. It was also a possible reason that it worked at all. To test this theory all the membranes were tested using the same set-up as before (1.5 cm^2 1.5 mg_{Pt}/cm^2 electrode, Kapton®-film with 1 cm^2 window and IL-PBI membranes) except only substituting doping with PA instead doping with 1 drop of corresponding IL. One drop IL was placed on each side of the membrane and then the MEA was assembled. Here the impedance spectra did not result in stable measurements and could not be analysed, see Appendix A5. This is a strong suggestion that what gave the IL-PBI their conductivity in these tests were the PA added.

4.3 General discussion

Overall, it does seem that the experiments have given valuable results. The methodology has been validated to literature and most experiments have followed a clear trend. At the same time, there are some uncertainties that need to be addressed. Firstly, the single cell tests of the IL-PBI could give more important information about the membrane in working conditions with a more extensive study going forward such as more activation of cells or more extensive characterization techniques. Secondly, the membranes have been casted by hand and do have some irregularities such as deviating thickness, colour and possibly even some solvent residuals. This could most likely have an impact on the results. Moreover, the IL-PBI membranes did not seem to work well enough without the addition of PA, even when adding liquid IL, which begs the question if the results shown in conductivity tests, impedance and polarisation tests are not really the results of IL-PBI membranes but actually the results of the added PA to these membranes.

The IL-PBI membranes were doped with as much PA for every experiment (0.038g) and a clear, repeatable distinction was seen between the different IL-PBI membranes. This could mean that the membranes have some different characteristics but need to be amplified by the PA. Else, this could mean that the different IL-PBI membranes have different interaction with PA and it is still the PA doing most of the conducting. With that said, an exact amount of PA in the membranes was not measured, only estimated, and the actual amount of PA in the membranes can vary. The estimated amount of PA per repeating PBI unit were 12.7, 10.7 and 7.9 respectively for [FA][TFSI]-PBI, [HEIm][TFSI]-PBI and [dema][TfO]-PBI. Comparing that to PA-PBI that have 10.2 PA per repeating PBI unit, they have similar amounts. With those amounts of PA the IL-PBI membranes should do better. This means that the membranes probably have not been doped fully or that there is some other reason the membranes still conduct poorly.

The results from all the tests done are that none of the PA doped IL-PBI membranes are close to being an alternative to PA doped PBI as of today. It is clear, however, that [FA][TFSI]-PBI is a better membrane when it comes to conductivity through-plane than the other two IL-PBI membranes in this report. This is evident by looking at the polarisation curve, Figure 12, and the Nyquist plot, Figure 15. On the other hand, the [FA][TFSI]-PBI membrane did not have as high in-plane conductivity as the [dema][TfO]-PBI membrane. This could be, as has been previously discussed, that the [FA][TFSI]-PBI membrane could have pores that are more suited for through-plane than in-plane conductivity. For example, the channels allow the PA to transfer the ions faster when operating in a cell. It could also be that the doping level of PA of the membrane varied between the tests. Since the PA was added by just placing a drop on top of the membrane and letting it be absorbed, the amount of acid in the membrane could vary. Nonetheless, [FA][TFSI]-PBI membrane had a current density of about 90 mA/cm^2 whereas [HEIm][TFSI]-PBI had 60 mA/cm^2 and [dema][TfO]-PBI had 25 mA/cm^2 while PA-PBI had a current density well over 1000 mA/cm^2. In other words, all IL-PBI membranes had a current density that was at least a factor ten less than PA-PBI. By comparison, the in cell HRF values from the EIS tests were 0.13, 0.39, 0.49 and 0.083 Ω for the membranes [FA][TFSI]-PBI, [dema][TfO]-PBI, [HEIm][TFSI]-PBI and PA-PBI respectively. These does not follow the same trend of the maximum current density and could mean different things; the HFR changes with applied load, or there are limitations in for example the electrodes due to the change in membrane properties. Both these aspects are of interest for future evaluation and deeper understanding of the membrane's properties.

Alashkar et.al [16] have made a summary of some of the IL-PBI membranes used today and their findings show that [dema][TfO]-PBI can have a conductivity of 20.7 mS/cm at 160 °C. Elwan et. al [31] found in their review that [dema][TfO]-PBI had a conductivity of 13.3 mS/cm. These values correspond very well with the through-plane conductivity of the PA doped [dema][TfO]-PBI from this study that was 26 mS/cm. The in-plane was measured to be 8.3 mS/cm for the same membrane which is lower than what could be found in the literature. Given that the membranes in this report were doped with PA these should be higher. At the same time, measurements from Chalmers suggest that the other two IL-PBI membranes, [FA][TFSI]-PBI and [HEIm][TFSI]-PBI, should have almost an insulator effect without addition of PA which is what could be seen in this report as well.

It seems like the PA has an important role in giving the membranes better performance. You could ask the question if a higher doping level of PA in the IL-PBI membranes could improve them. A concern of doping the IL-PBI membrane with PA is that the PA could replace the IL in the PBI membrane, that by adding PA it could make the membrane have less doping level of IL instead. Then it would be no different than PA-PBI. More research on how the IL-PBI membranes react to PA doping is needed to make any conclusions on this. Another concern is that the entire idea of using IL-PBI membranes is to get rid of the use of PA in HT-PEMFC.

5 Conclusions

The report shows that the tested IL-PBI membranes do not perform well as an electrolyte in HT-PEMFC as the PA-PBI membrane. Only when doped with one drop of PA does the membranes give any readable results and even then are the current densities a factor ten lower than the one of PA-PBI and the in-plane resistance a factor ten larger. The through-plane resistance, however, of the PA doped IL-PBI is 1.6 to 6 times larger than the one of PA-PBI which is not as bad but still not an improvement to today's technology.

The report shows that [dema][TfO]-PBI has the best in-plane conductivity, but it does not perform well in a fuel cell setting. [FA][TFSI]-PBI membrane shows the best through-plane conductivity with a margin, and it does also have the best performance in the polarisation tests. It does, however, only beat [HEIm][TFSI]-PBI membrane by a small margin in through-plane conductivity. Further studies are needed to give a better understanding of how IL-PBI work and how these can be used to optimise performance.

Some complications with the methodology were made that brings uncertainty to the test results. That the IL-PBI membranes did not get any activation before testing can be seen as an error source. At the same time does the conductivity test strengthen the results gotten from the single cell tests. It would probably be needed to run the IL-PBI membranes again, this time with activation to validate the results. The study also highlights the difficulty in analysing complex systems of multiple layers and materials by only measuring current and voltage which is important for further development of the fuel cell area.

6 References

1. IPCC, 2022: *Climate Change 2022: Impacts, Adaptation, and Vulnerability*. Contribution of Working Group II to the Sixth Assessment Report of the Intergovernmental Panel on Climate Change [H.-O. Pörtner, D.C. Roberts, M. Tignor, E.S. Poloczanska, K. Mintenbeck, A. Alegría, M. Craig, S. Langsdorf, S. Löschke, V. Möller, A. Okem, B. Rama (eds.)]. Cambridge University Press. Cambridge University Press, Cambridge, UK and New York, NY, USA, 3056 pp., doi:10.1017/9781009325844.
2. Haroff, K., & Hartis, J. (2008). Climate Change and the Courts: Litigating the Causes and Consequences of Global Warming. *Natural Resources & Environment*, *22*(3), 50–55. http://www.jstor.org/stable/40924928
3. Gittleman, C. S., Jia, H., De Castro, E. S., Chisholm, C. R. I., & Kim, Y. S. (2021). Proton conductors for heavy-duty vehicle fuel cells. *Joule*, *5*(7), 1660-1677. https://doi.org/10.1016/j.joule.2021.05.016
4. Hannah Ritchie, Max Roser and Pablo Rosado (2020) - "CO_2 and Greenhouse Gas Emissions". Published online at OurWorldInData.org. Retrieved from: 'https://ourworldindata.org/co2-and-greenhouse-gas-emissions' [Online Resource]
5. Hydrogen. (n.d.). *Hyundai*. https://www.hyundai.com/eu/mobility-and-innovation/hydrogen-energy/hydrogen.html
6. Toyota EU. (n.d.). *Toyota Fuel Cell Electric Vehicles | Toyota Europe*. https://www.toyota-europe.com/electrification/fcev
7. Volvo Trucks showcases new zero-emissions truck. (2022). *Volvo Group*. https://www.volvotrucks.com/en-en/news-stories/press-releases/2022/jun/volvo-trucks-showcases-new-zero-emissions-truck.html
8. Guillot, D. J., European Parliament (2023). “Reducing car emissions: new CO2 targets for cars and vans explained”. Published online at https://www.europarl.europa.eu/news/en/headlines/society/20180920STO14027/reducing-car-emissions-new-co2-targets-for-cars-and-vans-explained.
9. United Nations. (n.d.). *Home - United Nations Sustainable Development*. United Nations. https://www.un.org/sustainabledevelopment/
10. Sundén, B. (2019). Electrochemistry and thermodynamics. In *Hydrogen, Batteries and Fuel Cells*. https://doi.org/10.1016/b978-0-12-816950-6.00002-6
11. Sanad, M. F., & Sreenivasan, S. T. (2022). Metal-organic framework in fuel cell technology: Fundamentals and application. In *Electrochemical Applications of Metal-Organic Frameworks* (pp. 135-189). https://doi.org/10.1016/b978-0-323-90784-2.00001-0
12. East, A. L. L., Nguyen, C. M., & Hempelmann, R. (2023). A 2023 update on the performance of ionic-liquid proton-exchange-membrane fuel cells. *Frontiers in Energy Research*, *11*. https://doi.org/10.3389/fenrg.2023.1031458
13. Zhang, J., Zhang, H., Wu, J., & Zhang, J. (2013). PEM Fuel Cell Fundamentals. In *Pem Fuel Cell Testing and Diagnosis* (pp. 1-42). https://doi.org/10.1016/b978-0-444-53688-4.00001-2
14. Hydrogen Storage. (2017). *US Department of Energy*. https://www.energy.gov/eere/fuelcells/articles/hydrogen-storage-fact-sheet
15. Shih, C. F., Zhang, T., Li, J., & Bai, C. (2018). Powering the Future with Liquid Sunshine. *Joule*, *2*(10), 1925-1949. https://doi.org/10.1016/j.joule.2018.08.016
16. Alashkar, A., Al-Othman, A., Tawalbeh, M., & Qasim, M. (2022). A Critical Review on the Use of Ionic Liquids in Proton Exchange Membrane Fuel Cells. *Membranes (Basel)*, *12*(2). https://doi.org/10.3390/membranes12020178
17. Seng, L. K., Masdar, M. S., & Shyuan, L. K. (2021). Ionic Liquid in Phosphoric Acid-Doped Polybenzimidazole (PA-PBI) as Electrolyte Membranes for PEM Fuel Cells: A Review. *Membranes (Basel)*, *11*(10). https://doi.org/10.3390/membranes11100728
18. Pingitore, A. T., Huang, F., Qian, G., & Benicewicz, B. C. (2019). Durable High Polymer Content m/p-Polybenzimidazole Membranes for Extended Lifetime Electrochemical Devices. *ACS Applied Energy Materials*, *2*(3), 1720-1726. https://doi.org/10.1021/acsaem.8b01820

19. Kannan, A., Aili, D., Cleemann, L. N., Li, Q., & Jensen, J. O. (2020). Three-layered electrolyte membranes with acid reservoir for prolonged lifetime of high-temperature polymer electrolyte membrane fuel cells. *International Journal of Hydrogen Energy*, *45*(1), 1008-1017. https://doi.org/10.1016/j.ijhydene.2019.10.186
20. Bagher Karimi, M., Hooshyari, K., Salarizadeh, P., Beydaghi, H., V.M. Ortiz- Martínez, A. Ortiz, I. Ortiz Uribe, Mohammadi, F., (2021) *A comprehensive review on the proton conductivity of proton exchange membranes (PEMs) under anhydrous conditions: Proton conductivity upper bound*, International Journal of Hydrogen Energy,Volume 46, Issue 69, 2021, Pages 34413-34437, ISSN 0360-3199, https://doi.org/10.1016/j.ijhydene.2021.08.015
21. Kallem, P., Eguizabal, A., Mallada, R., & Pina, M. P. (2016). Constructing Straight Polyionic Liquid Microchannels for Fast Anhydrous Proton Transport. *ACS Appl Mater Interfaces*, *8*(51), 35377-35389. https://doi.org/10.1021/acsami.6b13315
22. Aili, D., Henkensmeier, D., Martin, S., Singh, B., Hu, Y., Jensen, J. O., Cleemann, L. N., & Li, Q. (2020). Polybenzimidazole-Based High-Temperature Polymer Electrolyte Membrane Fuel Cells: New Insights and Recent Progress. *Electrochemical Energy Reviews*, *3*(4), 793-845. https://doi.org/10.1007/s41918-020-00080-5
23. McNeice, P., Marr, P. C., & Marr, A. C. (2021). Basic ionic liquids for catalysis: the road to greater stability. *Catalysis Science & Technology*, *11*(3), 726-741. https://doi.org/10.1039/d0cy02274h
24. Niu, B., Luo, S., Lu, C., Yi, W., Liang, J., Guo, S., Wang, D., Zeng, F., Duan, S., Liu, Y., Zhang, L., & Xu, B. (2021). Polybenzimidazole and ionic liquid composite membranes for high temperature polymer electrolyte fuel cells. *Solid State Ionics*, *361*. https://doi.org/10.1016/j.ssi.2021.115569
25. Zhang, J., Zhang, H., Wu, J., & Zhang, J. (2013). Fuel Cell Open Circuit Voltage. In *Pem Fuel Cell Testing and Diagnosis* (pp. 187-200). https://doi.org/10.1016/b978-0-444-53688-4.00007-3
26. Carlson, A. (2019). *Electrochemical properties of alternative polymer electrolytes in fuel cells* (PhD dissertation, KTH Royal Institute of Technology). Retrieved from http://urn.kb.se/resolve?urn=urn:nbn:se:kth:diva-263095
27. Magar, H. S., Hassan, R. Y. A., & Mulchandani, A. (2021). Electrochemical Impedance Spectroscopy (EIS): Principles, Construction, and Biosensing Applications. *Sensors (Basel)*, *21*(19). https://doi.org/10.3390/s21196578
28. Ma, Y. L., Wainright, J. S., Litt, M. H., & Savinell, R. F. (2004). Conductivity of PBI Membranes for High-Temperature Polymer Electrolyte Fuel Cells. *Journal of The Electrochemical Society*, *151*(1). https://doi.org/10.1149/1.1630037
29. Nur Anati Bazilah Daud (2022) J. Phys.: Conf. Ser. 2259 012021
30. Parrondo, J., Venkateswara Rao, C., Ghatty, S. L., & Rambabu, B. (2011). Electrochemical Performance Measurements of PBI-Based High-Temperature PEMFCs. *International Journal of Electrochemistry*, *2011*, 1-8. https://doi.org/10.4061/2011/261065
31. Elwan, H. A., Mamlouk, M., & Scott, K. (2021). A review of proton exchange membranes based on protic ionic liquid/polymer blends for polymer electrolyte membrane fuel cells. *Journal of Power Sources*, *484*. https://doi.org/10.1016/j.jpowsour.2020.229197

7 Appendix

7.1 Individual impedance data

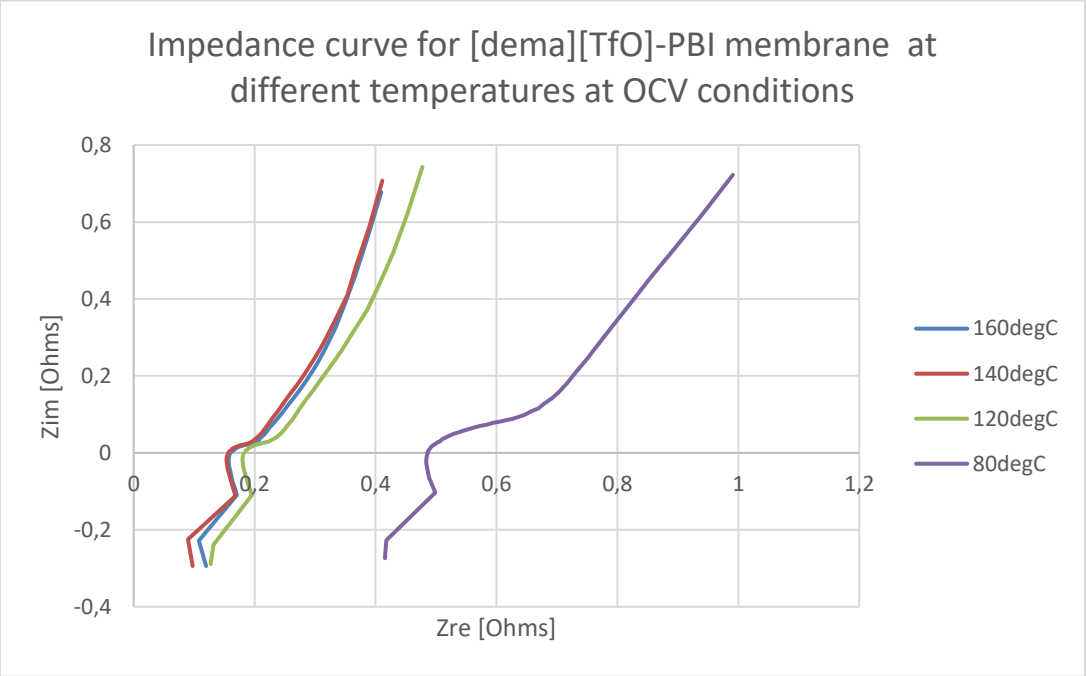

Figure A1. A graph showing the impedance curve of the first test of a cell with a PBI membrane, doped with [dema][TfO], and 3 drops (~0.114g) of PA on each electrode measured at the temperatures 160℃, 140℃, 120℃, 80℃ at open current voltage conditions.

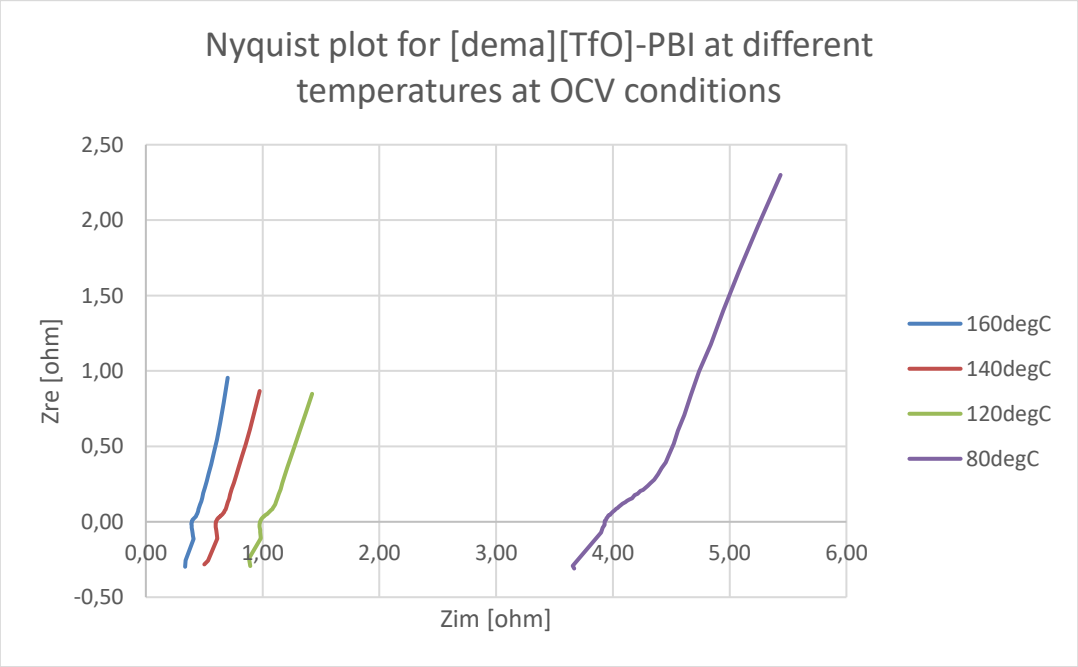

Figure demaImp2. A graph showing the impedance curve of the second test of a cell with a PBI membrane, doped with [dema][TfO], and 1 drop (~0.038g) of PA on each electrode measured at the temperatures 160℃, 140℃, 120℃, 80℃ at open current voltage conditions.

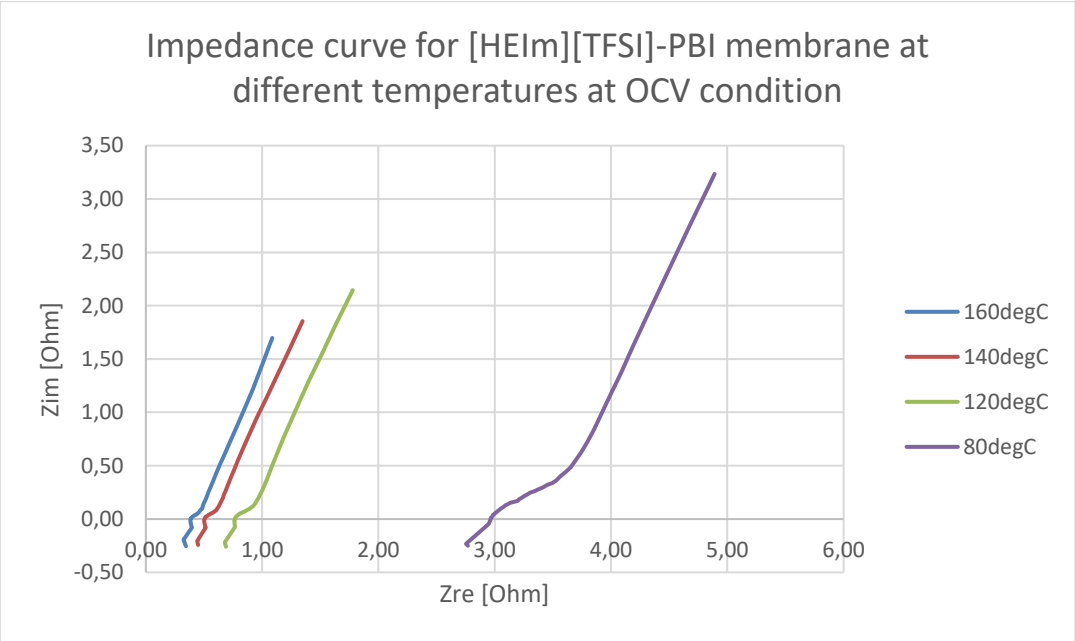

Figure A2. A graph showing the impedance curve of the first test of a cell with a PBI membrane, doped with [HEIm][TFSI], and 1 drop (~0.038g) of PA on each electrode measured at the temperatures 160℃, 140℃, 120℃, 80℃ at open current voltage conditions.

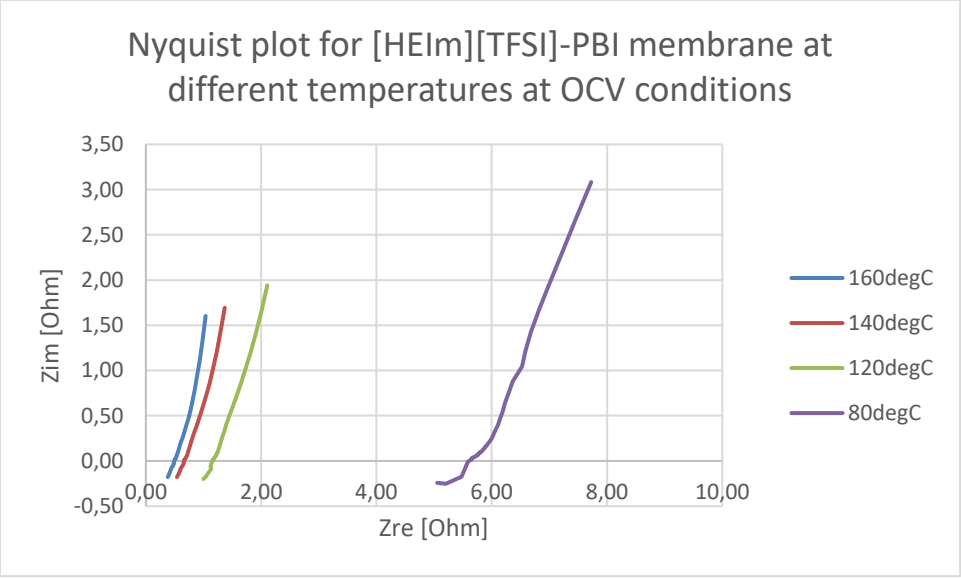

Figure A3. A graph showing the impedance curve of the second test of a cell with a PBI membrane, doped with [HEIm][TFSI], and 1 drop (~0.038g) of PA on each electrode measured at the temperatures 160℃, 140℃, 120℃, 80℃ at open current voltage conditions.

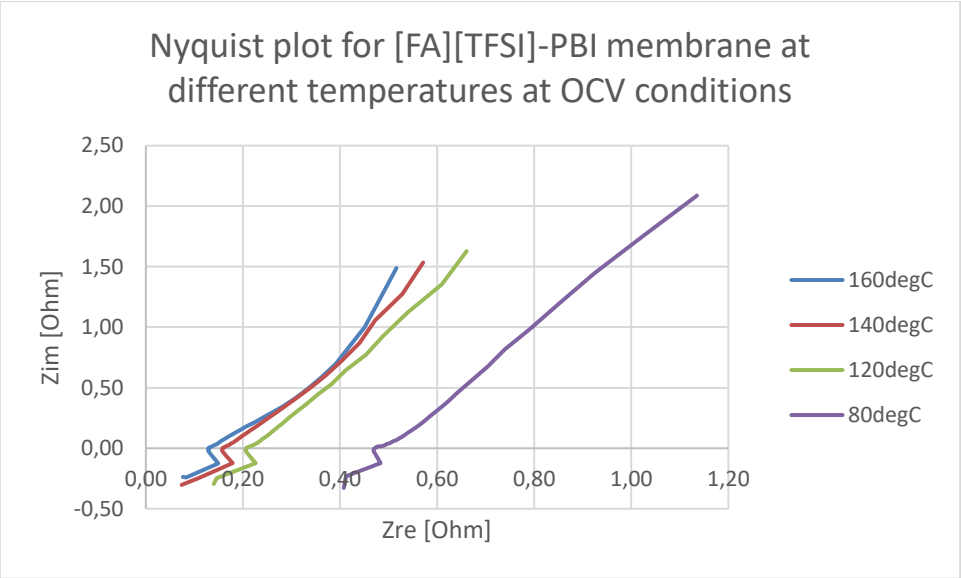

Figure A4. A graph showing the impedance curve of the second test of a cell with a PBI membrane, doped with [FA][TFSI], and 1 drop (~0.038g) of PA on each electrode measured at the temperatures 160℃, 140℃, 120℃, 80℃ at open current voltage conditions.

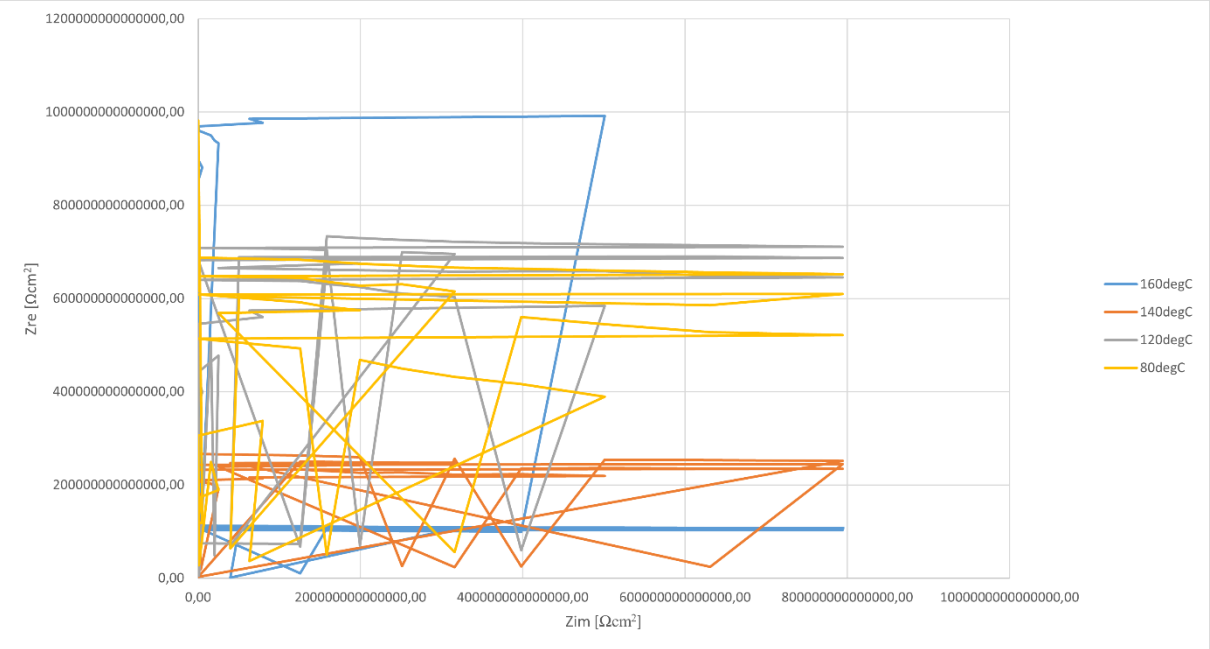

Figure A5. Nyquist plot of [dema][TfO]-PBI membrane with a drop of [dema][TfO] at both sides of the membrane at different temperature.